Studies on Neuropilin-1 in cancer

- VEGF-A promotes cancer cell proliferation and invasion by an autocrine mechanism –

2015

Ayumi Yoshida

Chapter 2.
VEGF-A/Neuropilin-1 signaling activates RhoA and promotes cancer cell invasiveness and metastasis.

General introduction

Vascular endothelial growth factor A (VEGF-A), a soluble glycoprotein, has been identified by N. Ferrara as a mitogen for vascular endothelial cells and induces signals of survival, migration, lumen formation, and the vascular permeability[1]. The human genome contains five genes encoding five distinct VEGF family members, VEGF-A, Placenta growth factor (PlGF), VEGF-B, VEGF-C, and VEGF-D. VEGF-A contains isoforms such as VEGF-A_{121}, VEGF-A_{165}, and VEGF-A_{189}[2]. VEGF-A has capability to induce physiological and pathological angiogenesis. Many malignant tumors secrete VEGF-A to induce blood vessels into tumors for supplying oxygen and nutrients, consequently promote cancer cell proliferation, survival and metastasis. Various studies have been implicated the relationship between up-regulation of VEGF-A and the poor prognosis in cancer patients[3].

VEGF-A has two tyrosine kinase receptors, VEGFR1 and VEGFR2 expressed in endothelial cells and transmit angiogenic signals. Avastin (Roche, Genentech) is a blockade of VEGF-A-VEGFRs binding and inhibits signals in vascular system to suppress tumor angiogenesis. Avastin was approved in metastatic colorectal cancer, non-small cell lung cancer (NSCLC), metastatic breast cancer, glioblastoma and ovarian cancer when combined with chemotherapy in Japan (Ministry of Health, Labor and Welfare, 2013). However, the impact on overall survival of the cancer patients has not been well documented. There have been several implications in literatures on the expression of VEGF receptors in cancer cells themselves which obtain also benefits from VEGF-A signaling by autocrine signaling loops (NSCLC, colorectal cancer and breast cancer)[4].

NRP1, a 130 kDa single-transmembrane protein, has been identified as a class 3 Semaphorins and VEGF receptor[5]. A striking feature of NRP1 is that it binds VEGF-A_{165} but not VEGF-A_{121}, making it isoform-specific. The structural difference between VEGF-A_{165} and VEGF-A_{121} is the 44 amino acids encoded by VEGF exon 7[6]. The binding of VEGF-A_{165} to NRP1 occurs via VEGF-A exon 7 in contrast to VEGFR1 and VEGFR2, which bind to VEGF-A_{165} via VEGF exon 4 and 3, respectively. NRP1 is expressed in various types of cell, including neuronal cells, endothelial cells and cancer cells. Neuropilin-1 (NRP1) is highly expressed in lung, brain, colon, ovarian and prostate

cancer with poor prognosis[6]. In endothelial cells, the function is a co-receptor of VEGFR2 to enhance VEGF-A binding to the receptor and modify the downstream signaling. Physiologically, NRP1 is crucial for vascular development. NRP1 deficient mice are lethal at 13.5 day due to impaired vasculogenesis[7]. Whereas pathologically, NRP1 act as a reservoir for VEGF-A supplying to peritumoral blood vessels and promotes no limited angiogenesis[8]. Although most studies on VEGF-A and VEGF receptors have been focused on their functions in angiogenesis in endothelial cells, the contribution of NRP to tumor progression has been shown recently by the observation that anti-NRP1 antibodies enhance the anti-tumor effects of anti-VEGF antibodies (Avastin)[5,48]. Recently, several reports indicated that NRP1 expressed cancer cells, such as in renal cell carcinoma, glioma and medulloblastoma, could transduces VEGFR2-independent signals and enhanced the tumorigenicity by autocrine manner[9-11].

The NRP1 extracellular B domain binds to VEGF-A_{165} via the domain encoded by exons 7 and 8 regions while VEGFR2 bind to the exons 3 and 4-coded regions of VEGF-A_{165}, which are also recognized by Avastin. Indeed, in AVAGAST, a phase III study to evaluate combinational effect of Avastin plus chemotherapy for patients with advanced gastric cancer, patient group with high expression of tumor NRP1 showed worse tendency in the overall survival compared to patients with the low baseline expression[12].

Structurally, NRP1 has a short cytoplasmic region consisting 44 amino acids and lacks kinase activity, so there has been a large effort to understand how NRP1 transduce the signals. Cao et al., Beck et al. and Snuderl et al. demonstrated tumor-NRP1 promotes cancer progressive signals, however, virtually nothing is known about the downstream signaling mechanisms by which VEGF-A/NRP1 regulates proliferative and invasive activity in any cancer types[9,11,13].

To elucidate The VEGF-A/NRP1 signaling, I used skin cancer, prostate cancer and glioblastoma cells throughout. In Chapter 1, I present a first detailed map of the VEGF-A-stimulated NRP1 signaling pathway leading to RhoA activation and cancer cell proliferation in which GIPC1 (GAIP interacting protein C terminus) plays a novel role in activating Syx, a RhoA activator. Importantly, the cell-penetrating peptide that competitively inhibits the interaction between GIPC1 and Syx was able to suppress cancer cell proliferation. In Chapter 2, I demonstrated VEGF-A/NRP1 signal not only

promotes cancer cell proliferation but also accelerates cancer metastasis. Taken together, the NRP1 C-terminal amino acids, SEA, is essential to induce GIPC1 interaction with Syx that is a key factor for RhoA activation, resulting in cancer cell invasion and metastasis.

Several reports have shown that NRP1/GIPC1 or GIPC1/Syx interaction occurs in angiogenesis. However, whether these interactions have a role in cancers cells has been unclear. This study provided new cancer progression mechanisms promoted by VEGF-A/NRP1 signaling pathway. Additionally, many researchers in the world have advocated targeting the extracellular domain of NRP1 to inhibit tumor angiogenesis, but in the present study, I suggested that targeting NRP1 cytoplasmic region may be more useful for anti-cancer therapy. This study will be particularly intriguing because VEGF-A/NRP1 and the downstream signaling may be especially useful for developing on molecular targeting cancer drug therapies.

Chapter 1.

VEGF-A/NRP1 stimulates GIPC1 and Syx complex formation to promote RhoA activation and proliferation in skin cancer cells.

1-1. Introduction

Malignant tumors express vascular endothelial growth factor A (VEGF-A), a glycoprotein that recruits blood vessels, thereby supplying tumors with the oxygen and nutrients that promote tumor cell migration, proliferation, survival, permeability and metastasis[3]. VEGF-A VEGF-A signaling involves via two tyrosine kinase receptors, VEGFR1 and VEGFR2. A previous study demonstrated that the blockade of VEGF-A by Avastin, an antibody or blockade of VEGFR2 with a specific kinase inhibitor such as Sutent, suppressed tumor angiogenesis[3].

Avastin, in combination with chemotherapy, has exhibited some efficacy in clinical trials for metastatic colorectal cancer, non-small cell lung cancer, renal cell carcinoma and metastatic breast cancer[14,15]. However, its impact on overall survival is not well documented.

Neuropilin-1 (NRP1) is a 130 kDa transmembrane protein that has been identified as a novel VEGF-A receptor[5]. NRP1 is expressed by endothelial cells and functions as a co-receptor of VEGFR2, enhancing VEGF-A binding to its receptor and promoting downstream signaling, e.g. MAPK pathway[16]. NRP1 is associated with tumor progression; it is strongly expressed in lung, brain, colon, ovarian and prostate cancer with poor patient prognosis[6]. A Phase III study to evaluate the combined effect of Avastin and chemotherapy in patients with advanced gastric cancer reported that overall survival was worse in patient groups that strongly expressed tumor NRP1 than

in patients with low baseline expression levels[12], suggesting that NRP1 is tumorigenic.

Structurally, NRP1 has two extracellular domains, a1a2 and b1b2, that bind SEMA3s and VEGF respectively, in addition to a dimerization domain, transmembrane domain and short cytoplasmic region[6]. Since NRP1 lacks kinase activity, there has been a concerted effort to elucidate the mechanisms underlying NRP1 signaling. NRP1 possesses a short cytoplasmic region of 44 amino acids that is involved in signaling. To date, the expression of NRP1 by tumor cells has been shown to contribute to proliferative signal transduction from VEGF-A. In renal cell carcinoma, the VEGF-A/NRP1 signal was found to activate Ras and promote tumor growth *in vivo*[9], while VEGF-A/NRP1 signals induced the phosphorylation of Akt leading to breast cancer cell survival[17]. However, the precise mechanisms responsible for molecular interactions with the NRP1 cytoplasmic region remain unknown.

NRP1 lacking the C-terminus three amino acids (Ser-Gln-Ala [SEA]) led to impaired vasculogenesis in zebrafish[18] and abnormal vascular remodeling during retinal development in mice[19]. A previous study showed that NRP1ΔSEA did not induce medulloblastoma tumorigenesis[11]. NRP1 appears to signal via the SEA region.

GIPC1 (GAIP interacting protein C terminus) a scaffold protein, is the first reported molecule that was shown to interact with the NRP1 cytoplasmic region[20,21]. It has a PDZ domain that binds to the SEA of NRP1[22,23]. GIPC1 is overexpressed in breast and pancreatic tumors and promotes tumor proliferation, survival and metastasis[24-26]; however, its function have yet to be determined in detail[27]. Syx was identified as a GIPC1 binding protein by a yeast two-hybrid system[28,29]. Syx found to bind to the GIPC1 PDZ domain via its C-terminus amino acids[30]. It has a RhoGEF domain and activates a Rho family GTPase, specifically, RhoA. Previous studies demonstrated that Syx was expressed in vascular endothelial cells, neuronal cells and some tumors, such as glioma cells[30-32]. RhoA drives the cell cycle into the S-phase[33]. RhoA has been implicated in virtually all stages of cancer progression. It may play a role during tumor cell proliferation and survival; for example, *in vitro*, constitutively active RhoA stimulate transformation[34]. The activation of RhoA is known to induce the protein degradation of $p27^{kip1}$, a cyclin dependent kinase inhibitor (CDI), in the G1 phase, which progresses the cell cycle, resulting in proliferation[35,36].

In the present study, we showed that VEGF-A promoted tumor cell proliferation via the NRP1 signaling pathway. The NRP1 cytoplasmic region was found to be essential

for the transduction of VEGF-A signaling, which enhanced interaction with GIPC1. GIPC1 subsequently formed a complex with Syx. This complex formation activated the RhoGEF activity of Syx, which led to the activation of RhoA. The downstream signaling of RhoA induced p27 protein degradation, leading to S phase entry of the cell cycle, resulting in cancer cell proliferation. A treatment with a cell-penetrating peptide designed to inhibit interactions between GIPC1 and Syx suppressed the activation of RhoA as well as cancer cell proliferation.

In summary, we proposed a novel signal transduction pathway of VEGF-A/NRP1 that induced cancer cell proliferation by forming a GIPC/Syx complex that activated RhoA and degraded p27.

1-2. Materials and Methods

1-2-1. Materials

Recombinant human-VEGF-A_{165}, VEGF-A_{121} and PlGF-2 were purchased from R&D Systems (Minneapolis, Minnesota, USA). The VEGFR kinase inhibitor SU5614 was purchased from Merck (Whitehouse Station, New Jersey, USA). The RhoA-specific inhibitor, C3 exoenzyme, was purchased from Cytoskeleton (Denver, Colorado, USA) and Y27632 was purchased from EMD Millipore (Billerica, Massachusetts, USA). The anti-VEGF-A antibody, Avastin® (bevacizumab), was kindly provided by Dr. Mark Kieran (Dana-Farber Cancer Institute, Boston, MA).

1-2-2. Animal studies

All animal experiments were performed in accordance with Kyoto Sangyo University's animal experiment guidelines. DJM-1 cells (4×10^6 cells per 100 µl HBSS) were orthotopically inoculated at the right flank of 6-week- old female BALB/C Slc-nu/nu mice (SHIMIZU Laboratory Supplies Co., Ltd., Sakyo-ku Kyoto, Japan). After 2 weeks, mice were sacrificed and tumors were isolated and embedded in OCT compound (SAKURA Tissue Teck, Koto-ku, Tokyo, Japan).

1-2-3. Cell culture and transfection

The human skin cancer line, DJM-1 was kindly provided by Dr. H. Katayama[37] (Katayama clinic, Maebashi, Japan) and cultured in DMEM supplemented with 10% fetal bovine serum (FBS) and glucose (final 4.5 mg/ml). HEK293T cells were purchased from ATCC and cultured in DMEM supplemented with 10% FBS. PC3M cells and U87MG cells were purchased from ATCC and cultured in RPMI-1640 supplemented with 10% FBS for PC3M cells. U87MG cells were cultured in EMEM supplemented with 10% FBS. Human Umbilical Vein Endothelial Cells (HUVEC) were purchased from LONZA (Gampel, Valais, Switzerland) and maintained in endothelial cell growth medium (EGM-2).

The transfection of expression vectors into HEK293T was performed with FuGENE6 (Promega, Madison, Wisconsin, USA). SiLentFect™ reagents (Bio-Rad, Hercules, CA, USA) were used for all siRNA treatments as directed in the instruction manual.

1-2-4. Antibodies

The following primary antibodies were used: GIPC1 (N-19) goat; neuropilin-1 (C-19) goat; neuropilin-1 (A-12) mouse; PLEKHG5 (KB-7) mouse; Flt-1 (C-17) rabbit and Flk-1

(C-1158) rabbit antibody (Santa Cruz, Dallas, Texas, USA); Akt (pan) (C67E7) rabbit; phospho-Akt (Ser473) (D9E) XP^{TM} rabbit; p44/42 MAPK (Erk1/2) rabbit; phospho-p44/42 MAPK (Erk1/2) (Thr202/Tyr204) rabbit; neuropilin-1 (D62C6) rabbit and RhoA (67B9) rabbit antibody (Cell Signaling Technology, Danvers, Massachusetts, USA). An anti-HA 11 clone (16B12) mouse antibody was purchased from Covance (Princeton, New Jersey USA). An anti-V5 rabbit antibody was purchased from Bethyl (Montgomery, Texas, USA). An anti-mouse CD31 (PECAM-1) (MEC 13.3) antibody was purchased from BD Biosciences Pharmingen (Franklin Lakes, New Jersey, USA). An anti-actin rabbit antibody (Cat: A2013) was purchased from Sigma-Aldrich (St. Louis, Missouri, USA).

The secondary antibodies used were: horseradish peroxidase (HRP)-conjugated anti rabbit IgG; HRP-conjugated anti goat IgG; HRP-conjugated anti-mouse IgG antibody (Jackson Immuno Research, West Grove, Pennsylvania, USA). DAPI was purchased from Invitrogen (Life Technologies, Van Allen Way, Carlsbad, CA, USA). A biotin-conjugated rat IgG antibody was purchased from VECTOR (Burlingame, CA, USA).

1-2-5. Plasmids

The human NRP1 WT, HA-tagged GIPC1, V5-tagged Syx, HA-tagged constitutively active RhoA, and soluble NRP constructs were inserted using pcDNA 3.1 TOPO expression vector (Life Technologies, Van Allen Way, Carlsbad, USA). HALO- tagged Syx was purchased from the Kazusa DNA Research Institute (KIAA0720) and used as a template to generate the V5-tagged Syx construct. The human NRP1ΔSEA construct was generated by PCR using NRP1WT as a template and primers that introduced NotI or BamHI restriction site were inserted into pcDNA 3.1 TOPO expression vector.

Forward primer; 5’-GGGCGGCCGCACCACCATGGAGAGGGGGCTGCCGCTCCTC-3’,

Reverse primer; 5’- GGGGATCCTCATGCCTCCGAATAAGTACTCT -3’.

Syx WT and a dominant negative mutant were generated by point mutations using the following primers;

Forward primer; 5’-CCAAGTACCCGCTGGAGCTCAAGTCGGTGC-3’,

Reverse primer; 5’-GCACCGACTTGAGCTCCAGCGGGTACTTGG-3’.

PCR products were digested with NotI and BamHI to insert into pcDNA 3.1 expression vectors.

NRP1 WT, NRP1ΔSEA and NRP1ΔCyto lentivirus were based on the NRP1 pcDNA 3.1

construct and generated by PCR, using the following primers that introduced NotI and BamHI restriction sites. The same primer for all NRP1 constructs was used as forward primer and PCR products were subcloned into the pHAGE lentiviral backbone vector as described above[38].

Forward primer; 5'-GGGCGGCCGCGCCACCATGGAGTGGGGGCTGCCGCTC -3',

Reverse primer; WT: 5'-CCGGATCCCTCTGTCTGCCTTCATGCCTC-3', ΔSEA: 5'-AAGGATC CTCAATAAGTACTCTGTGTATTCAGTTTGTC-3' and ΔCyto: 5'-GGGGATCCTCAGTACAGCAC GACCCCACAGAC-3'.

Syx WT or DN-V5 tagged lentivirus was based on each pcDNA 3.1 construct and generated by PCR using the following primers that introduced the NotI or BamHI restriction site. PCR products were subcloned into the pHAGE lentiviral backbone vector.

Forward primer; 5'-GCGGCCGCGCCACCATGGGTAAGCCTATCCCTAACCCTCTCCTCGGTCT -CGATTCTACGGGTGACGAGACCAGAGCCCCGCT-3',

Reverse primer; 5'-GGGGGATCCTCAGACCTCCGAGGCAGTGAGC-3'.

The following NRP1 shRNA sequences based on siNRP1 #3 were inserted into pSilencer^{TM} 4.1-CMV neo (Ambion; Life Technologies):

Sense primer;

5'-GATCCCGGGCTGAGGATTGTACAGTTCAAGAGACTGTACAATCCTCAGCCCGTCA-3',

Antisense primer;

5'-AGCTTGACGGGCTGAGGATTGTACAGTCTCTTGAACTGTACAATCCTCAGCCCGG-3'.

1-2-6. Preparation of Lentivirus vectors of NRP1 WT and mutants

Each NRP1WT, NRP1ΔSEA, and NRP1ΔCyto in the pHAGE lentiviral backbone vector was co-transfected with the helper plasmids (tat, rev, gag- pol and VSV-G) to HEK293 cells as described previously[38]. Viral supernatants were assembled and concentrated at 38,000×g for 1.5 h at 4°C. The collected virus was infected with 10 μg/ml polybrene (Millipore) to express NRP1WT and the mutants in DJM-1 cells.

1-2-7. siRNAs

siGENOME smart pool control siRNA (D-001206), GIPC1 siRNA (M-019997), and Syx siRNA (M-013873) were purchased from Dharmacon RNAi Technologies (Thermo Scientific, Waltham, Massachusetts, USA). Human VEGF-A siRNA #1, #2, and #3 were annealed using the following sequences, respectively;

VEGF-A siRNA #1; sense primer: 5'-GCAUUGGAGCCUUGCCUUGCUTT-3', antisense

primer: 5’-AGCAAGGCAAGGCUCCAAUGCTT-3’.

VEGF-A siRNA #2; sense primer: 5’-GGAGCCUUGCCUUGCUGCUCUTT-3’, antisense primer: 5’-AGAGCAGCAAGGCAAGGCUCCTT-3’.

VEGF-A siRNA #3; sense primer: 5’-GGACCUAUGUCCUCACACCTT-3’, antisense primer: 5’-GGUGUGAGGACAUAGGUCCTT-3’.

Human NRP1 siRNA #1, #2, and #3 were annealed using the following sequences, respectively; NRP1 siRNA #1; sense primer: 5’-AAUCAGAGUUUCCAACAUATT-3’, antisense primer: 5’-UAUGUUGGAAACUCUGAUUTT-3’. NRP1 siRNA #2; sense primer: 5’-GUGGAUGACAUUAGUAUUATT-3’, antisense primer: 5’-UAAUACUAAUGUCAUCCAC-TT-3’. NRP1 siRNA #3; sense primer: 5’-GACGGGCUGAGGAUUGUACTT-3’, antisense primer: 5’-GUACAAUCCUCAGCCCGUCTT-3’.

1-2-8. shNRP1 construction and transfection

The designed shNRP1 oligonucleotide sequences were based on siNRP1 #3.

Sense oligo: 5’-GATCCCGGGCTGAGGATTGTACAGTTCAAGAGACTGTACAATCCTCAGCCC-GTCA-3’, antisense oligo: 5’-AGCTTGACGGGCTGAGGATTGTACAGTCTCTTGAACTGTACA-ATCCTCAGCCCGG-3’. The sense and antisense oligonucleotides were annealed and inserted at the BamHI and HindIII restriction sites into the pSilencerTM 4.1-CMV neo plasmid (Ambion; Life Technologies). DJM-1 cells were transfected with the shNRP1 construct or control plasmid by electroporation with a 0.4 cm cuvette (GenePulser Xcell; Bio-Rad). The transfectants were screened in 400 μg/ml G418-contained growth medium to obtain stable DJM-1 cell clones (shNRP1 clone #12 and #13, shControl).

1-2-9. Peptides

The expression plasmids for fusion proteins, TAT-EGFP-peptide 1 (STLTASEV) and TAT-EGFP-scramble 1 (EASTSLVT) were prepared by site-directed mutagenesis of DNA sequences encoding TAT-EGFP cloned in a pGEX-6P-3 expression vector (GE Healthcare Life Sciences, Buckinghamshire, UK)[39]. DNA primers for amplification of the plasmids were follows: for TAT-EGFP-peptide 1, 5´-GCCAGCGAGGTGTAAATCGTGACTGACTGACG-ATCTGCC-3´ and 5´-GGTCAGGGTGCTGCCCTTGTACAGCTCGTCCATGGCG-3´; for TAT-EGFP-scramble 1, 5´-AGCCTGGTGACCTAAATCGTGACTGACTGACGATCTGCC-3´ and 5´-GGTGCTGGCCTCGCCCTTGTACAGCTCGTCCATGGCG-3´;. The resultant plasmids were introduced into BL21-CodonPlus (DE3) cells (Agilent Technologies, Santa Clara, CA, USA). Fusion proteins were expressed as glutathione S-transferase (GST)-tagged proteins and purified by affinity chromatography as previously described[39]. The

GST-tag was removed and final proteins were equilibrated in PBS.

1-2-10. Membrane fractionation

DJM-1 cells were grown in two 100 mm cell culture dishes per sample at 80% confluency. The cells were washed three times with cold PBS and scraped with low salt homogenization buffer (300 mM HEPES-NaOH pH 7.4, 1 mM EDTA, protease inhibitor). The cells were transferred to a glass potter and homogenized in 3 ml buffer at 4,800 rpm on ice. The nuclei and cell debris were removed by centrifugation at 2,000 rpm at 4°C for 10 min. The resulting supernatant was further ultracentrifuged at 100,000 ×g at 4°C for 1 h. The membrane pellets were solubilized with RIPA buffer. Insoluble materials were removed by centrifugation at 15,000 rpm for 5 min at 4°C. Solubilized membrane proteins were analyzed by SDS-PAGE followed by Western blotting.

1-2-11. Co-Immunoprecipitation (IP)

HEK293T cells seeded at $3x10^5$ cells/6 cm dish were transfected with NRP1 WT, GIPC1 and Syx plasmids with FuGENE6. After 36 h incubation, cells were stimulated with or without 100 ng/ml VEGF-A for 15 min. Cells were washed three times with cold PBS and collected with a scraper. Collected cells were transferred and centrifuged at 15,000 rpm at 4°C for 5 min. Supernatant was discarded and cells were lysed with 300 μl RIPA buffer (1% NP-40, 0.5% Sodium Deoxycholate, 0.1% SDS, NaCl 100 mM, Tris-HCl 50 mM, pH7.4). After homogenized, the homogenate was centrifuged at 15,000 rpm at 4°C for 10 min. The cell lysates were transferred into a fresh centrifuge tube. For IP analysis, cell lysates were incubated with either 2 μl of anti-HA, anti-GIPC1 (N-19) or anti-Syx antibody at 4°C for overnight. PBS-equilibrated Protein G Sepharose (Protein G Sepharose 4 Fast Flow, GE Healthcare) was added and rotated at 4°C for 1.5 h to pull down antibodies. After washing the beads three times with cold RIPA buffer, proteins were removed from the beads in 40 μl 2xloading buffer and analyzed by SDS-PAGE and Western blot. For input analysis, 1/10 volume of cell lysate was used and normalized the amounts of binding NRP1, GIPC1 or Syx respectively. Each experiment was repeated three times.

1-2-12. Western Blotting

Cells were lysed with cold RIPA buffer. After running SDS-PAGE, proteins were transferred to a PVDF membrane (Millipore) and blotted with primary antibody-diluted 4% skim milk in TBST at 4°C overnight followed by incubation with a HRP-conjugated secondary antibody. The blots were treated with chemiluminescent substrate solution

(Thermo Fisher Scientific, Waltham, MA, USA) and exposed to LAS-4000 mini (Fujifilm Co., Tokyo, Japan) to reveal immunoreactive bands. Percentages from each band on densitometry compared to the control were indicated in the lower lanes in the figures. The western blot analysis was repeated 3 times.

1-2-13. VEGF-A ELISA

Human VEGF Quantikine® ELISA kit (R & D Systems) was used. DJM-1 cells were seeded at the density of $2x10^5$ cells/well/6-well plate, followed by treatment with 20 nM siRNA. The medium was changed to DMEM containing 1% BSA, and cells were incubated for 3 days. The conditioned media were diluted to ten-fold with serum free-DMEM, and VEGF-A levels were measured using the manufacturer's protocol.

1-2-14. Colony formation assay

DJM-1, PC3M, or U87MG cells were treated with 20 nM siRNA or infected with a lentivirus before being seeded in agar. Two milliliters of growth medium containing 0.72% agar was prepared in a 35-mm dish and solidified as bottom agar. Cells (DJM-1: $5×10^4$ cells, PC3M and U87MG: $1×10^5$ cells) were suspended in 2 ml of culture medium containing 0.36% agar and, after the addition of ligands or chemicals, layered on the bottom agar. Two weeks later, viable cells were stained with 300 μg/ml 3-(4,5-Dimethyl-2-thiazolyl)-2,5-diphenyl-2H-tetrazolium bromide (MTT) solution. Colony diameters were analyzed by Image J software and the numbers of colonies larger than 80 μm in diameter were counted per 6 to 7 microscopic fields. The means±s.d of colony numbers are shown. Percentages from each mean compared to the control are indicated below the graphs in the figures. Each experiment was repeated at least two or three times.

1-2-15. HUVEC migration assay

A migration assay was performed for HUVEC using Transwell inserts with a pore size of 8.0 μm (Corning, NY, USA). Membranes were coated with 0.1% gelatin. The conditioned medium of DJM-1 cells was prepared with a siRNA treatment, cultured in 2% FBS-EBM-2 for 72 h, and placed into the bottom chamber. Five thousand HUVEC were suspended in 2% FBS-EBM- 2 medium, seeded into the upper compartments, and cultured for 16 h. Migrated cells were stained with Diff-Quick. The stained cells in 6 microscopic fields were counted.

1-2-16. RhoA activity assay

RhoA activity assay was performed and quantified using the RhoA activation assay kit

based on rhotekin pull-down, according to the manufacturer's instructions (Cytoskeleton, Denver, Colorado, USA). DJM-1 cells were treated with 20 nM siRNA before use and were seeded in 5 mg/ml polyHEMA (poly 2-hydroxyethyl methacrylate; Sigma)-coated 100-mm dishes for cultivation under anchorage-independent conditions overnight[40]. Cells were stimulated with 100 ng/ml VEGF-A_{165} for 15 min or the indicated time. The cells were washed twice with cold PBS and lysed with Lysis buffer (50 mM Tris pH 7.5, 10 mM $MgCl_2$, 300 mM, NaCl, 2% IGEPAL). The clarified cell lysate was incubated with Rhotekin-RBD protein agarose beads and rotated at 4°C for 90 min. The beads were washed once with wash buffer (25 mM Tris pH 7.5, 30 mM $MgCl_2$, 40 mM NaCl), suspended in 2×loading dye (125 mM Tris HCl pH6.8, 20% glycerol, 4% SDS, 4% mercaptoethanol, 0.025% BPB) and run on a SDS-gel. Active RhoA was detected by Western blotting. The experiment was repeated three times and normalized by each total RhoA.

1-2-17. Statistical analyses

All numerical data were expressed as the mean±standard error of the mean (SEM). A one-way analysis of variance (ANOVA) followed by with post-hoc analysis. Differences of mean among treatments were evaluated with a two-tailed, paired Student's *t*-test, Bonferroni test and Tukey test in colony formation assay and ELISA. $^{\#}$, $^{\#\#}$, **, *** and N.S. stand for $P<0.05$, $P<0.01$, $P<0.005$, $P<0.001$ and "not significant", respectively.

1-3. Results

1-3-1. Knockdown of endogenous VEGF-A expression decreased human skin cancer cell proliferation *in vitro*.

The DJM-1 cell line was established from a human malignant skin cancer obtained from a patient who died from metastases to the axillary lymph nodes and lung. DJM-1 cells were orthotopically inoculated into the backs of mice. After 2 weeks, mice were sacrificed and the tumors were isolated. Tumor sections were stained with anti-CD31 antibody (Arrow: bv) and hematoxylin. The tumors and the peritumoral area were highly vascularized **(Fig. 1-1A).** The amounts of VEGF-A secreted into DJM-1 cell conditioned media (CM) were 8 ng/ml/72 h as measured by ELISA, while that secreted into siControl-treated DJM-1 cell CM were 7.5 ng/ml/72 h **(Fig. 1-1B).** VEGF-A was suppressed by knockdown using 3 different siRNAs, with siVEGF-A #1 being the most effective (siVEGF-A #1: 90% inhibition, siVEGF-A #2: 88 % inhibition, siVEGF-A #3: 65.4% inhibition, respectively) **(Fig. 1-1B).** VEGF-A secreted by DJM-1 cells stimulated migration of HUVEC. The knockdown of VEGF-A expression suppressed the migration of HUVEC (siVEGF-A #1: 38% and siVEGF-A#2: 48% of siControl, respectively) **(Fig. 1-1C).** Colony formation in soft agar indicated cancer proliferation under anchorage-independent conditions. The knockdown of VEGF-A expression suppressed the anchorage-independent proliferation (52% of siControl) of DJM-1 cells themselves **(Fig. 1-1D, E)**. The addition of exogenous VEGF-A (1 μg/ml) restored the proliferation of siVEGF-A-treated DJM-1 cells to a level similar to the siControl-treated cells (siVEGF-A#1 +1 μg/ml VEGF-A, 92% of siControl). These results suggest that endogenous VEGF-A expression stimulates the proliferation of DJM-1 cells in an autocrine manner.

1-3-2. VEGF-A-induced DJM-1 cell proliferation did not depend on VEGFR1 or VEGFR2.

VEGF-A has multiple receptors: VEGFR1, VEGFR2 and neuropilin 1 and 2[1]. The expression of VEGFR1 and VEGFR2 was detected by Western blotting in HUVEC, but not in DJM-1 cells **(Fig. 1-2A).** In order to determine whether VEGFR1 or VEGFR2 signaling occurred in DJM-1 cells in response to VEGF-A, the effect of SU5614, a VEGFR tyrosine kinase inhibitor, were tested on DJM-1 cells in soft agar **(Fig. 1-2B)**. However,

SU5614 did not inhibit the proliferation of DJM-1 cells (DMSO: 100%, SU5614: 96%). Avastin is an antibody that neutralizes VEGF-A and targets VEGFR-binding sites. However, Avastin did not inhibit DJM-1 cell proliferation (no addition: 100%, 1 μg/ml: 97%, 10 μg/ml: 96%, 250 μg/ml: 94%, respectively) **(Fig. 1-2C)**. These results suggested that the autocrine VEGF-A induced cancer proliferation, but does not mediate the VEGFR1 or VEGFR2 signaling pathway.

1-3-3. VEGF-A promoted cancer cell proliferation via NRP1 in an autocrine manner.

DJM-1 cells express only NRP1, but not NRP2. In addition, NRP1 siRNA (siNRP1) #1–3 almost completely abrogated protein expression (siNRP1 #1: 7%, #2: 4%, #3: 3% respectively), inhibiting DJM-1 cell anchorage-independent proliferation from 59 to 94% **(Fig. 1-3A, B)**. Since siNRP1 #2 was the most effective inhibitor of proliferation, it was used in subsequent experiments. The siNRP1 treatment inhibited the proliferation of DJM-1 cells, similar to siVEGF-A (siControl: 100%, siNRP1: 39%, siVEGF-A: 35%, respectively) **(Fig. 1-3C)**. The addition of exogenous recombinant VEGF-A did not rescue siNRP1-treated DJM-1 cell proliferation (42%), but it did rescue siVEGF-A-treated DJM-1 proliferation (96%) **(Fig. 1-3C)**. We also assessed the expression of NRP1 protein by western blotting and VEGF-A by ELISA in other human cancer cell lines: PC3M, prostate cancer and U87MG, glioblastoma **(Fig. 1-4A and B, Fig2-1A and B)**. NRP1 mRNA and protein (~130 kDa) were highly expressed in PC3M and U87MG **(Fig. 1-4A)**. All cell lines expressed NRP1, but did not express VEGFRs. U87MG cells expressed NRP1 and NRP2 **(Fig. 1-4A)**. U87MG cells secreted the highest levels of VEGF-A into conditioned medium, as shown in **Fig. 1-4A and Fig. 2-1B**. The siVEGF-A or siNRP1 treatment inhibited the proliferation of PC3M (siControl: 100%, siVEGF-A: 15%, siNRP1: 23%) and U87MG cells (siControl: 100%, siVEGF-A: 33%, siNRP1: 41%) **(Fig. 1-4C)**. The addition of exogenous VEGF-A rescued the proliferation of siVEGF-A-treated cells (PC3M: 77%, U87MG: 78%). In contrast, the addition of VEGF-A did not recover the proliferation of siNRP1-treated cells (PC3M: 38%, U87MG: 46%), suggesting that NRP1 mediated VEGF-A signaling to induce PC3M and U87MG cell proliferation as in DJM-1 cells **(Fig. 1-4C)**.

Soluble-NRP (sNRP) is a VEGF-TRAP, that consists of the NRP1 extracellular B domain, which is the NRP1 domain responsible for VEGF-A-binding via its exon 7- and 8-encoded regions[41]. sNRP inhibited DJM-1 cell proliferation in a dose-dependent

manner (20 ng/ml: 9% inhibition of no addition, 50 ng/ml: 42%, 100 ng/ml: 51%, respectively) **(Fig. 1-3D)**. VEGF-A_{165} is a major isoform of VEGF-A that containing exon 7 and 8 residues. VEGF-A_{121} is a spliced isoform of VEGF-A and lacks the residues encoded by exon 7. Therefore, NRP1 binds VEGF-A_{165} but not $VEGF_{121}$[42]. The addition of VEGF-A_{121} did not promote siVEGF-A treated DJM-1 cell proliferation. PlGF-2, a member of the VEGF family that has been shown to NRP1[43], promoted siVEGF-A-treated DJM-1 cell proliferation to 50% siControl (siControl: 100%, siVEGF-A: 21%, siVEGF-A +VEGF-A_{165}: 93%, siVEGF-A +VEGF-A_{121}: 21%, siVEGF-A +PlGF-2: 50%, respectively) **(Fig. 1-3E)**. These results suggested that NRP1 mediated VEGF-A signaling to promote DJM-1 cell proliferation.

1-3-4. The NRP1 cytoplasmic region was responsible for VEGF-A-induced proliferation of DJM-1 cells.

NRP1 does not have any known signaling motif in the short 44 amino acid cytoplasmic region; therefore, it currently remains unclear whether this domain is involved in signaling. We constructed a shNRP1 vector to abrogate the expression of NRP1 in DJM-1 cells. The sequence of shNRP1 was based on siNRP1 #3, which targeted NRP1 3'UTR. shNRP1 clones (No. 12 and No. 13) did not express NRP1 and also did not support DJM-1 cell proliferation (shControl: 100%, shNRP1-12: 33% , shNRP1-13: 15%, respectively) **(Fig. 1-5A)**. In subsequent experiments, we used shNRP1 clone No. 13 and infected shNRP1-DJM-1 cells clones with NRP1WT, NRP1 lacking the 44 amino acid cytoplasmic region (NRP1ΔCyto), or NRP1 lacking the C- terminus amino acids, SEA (NRP1ΔSEA). Growth of shNRP1 clone was inhibited compared to shControl clone (33% of shControl) **(Fig. 1-5A)**. The growth of the shNRP1 clone was less than that of the shControl clone (40% of shControl) **(Fig. 1-5C)**. The lentiviral overexpression of NRP1WT restored growth, whereas NRP1ΔSEA and NRP1ΔCyto did not (shNRP1+WT: 90%, shNRP1+ΔSEA: 27%, shNRP1+ΔCyto: 23%, respectively) **(Fig. 1-5C)**. These results suggested that the NRP1 cytoplasmic region, containing SEA, was essential for VEGF-A-induced proliferation.

1-3-5. VEGF-A binding to NRP1 induced the interaction between GIPC1 and Syx, thereby promoting DJM-1 proliferation.

GIPC1 (RGS-GAIP-interacting protein C-terminus) has a PDZ domain that interacts

with the NRP1 C-terminal three amino acid residues, SEA[18]. Syx has been shown to binds to the GIPC1 PDZ domain via its C-terminus[28,29]. NRP1, GIPC1 and Syx proteins were overexpressed in HEK293T cells, which did not express VEGFR1 or VEGFR2 **(Fig. 1-5D).**

A co-immunoprecipitation analysis (Co-IP) with GIPC1 (HA) showed that NRP1/GIPC1 and Syx/GIPC1 complexes were increased in the presence of VEGF-A (+) compared to those in the absence of VEGF-A (-) **(Fig 1-5Ea, asterisks)**. On the other hand, Co-IP with Syx showed that the GIPC1/Syx complex was increased, however, NRP1/Syx complex was less prominent in the presence of VEGF-A (+) than in its absence (-) **(Fig. 1-5Eb, asterisks)**. These results suggested that the VEGF-A/NRP1 induced GIPC1 binding to NRP1 and the formation of the GIPC1/Syx, which appeared to be released from NRP1.

In order to determine whether GIPC1 and Syx mediated the VEGF-A/NRP1 signal in DJM-1 cells, we treated DJM-1 cells with siGIPC or siSyx and analyzed the proliferation in the presence of exogenous VEGF-A. The siGIPC1 and siSyx treatments both reduced the expression of GIPC1 and Syx **(Fig. 1-5F)** and inhibited the proliferation of DJM-1 cells in the absence of exogenous VEGF-A **(Fig. 1-5G,** black columns, siControl: 100%, siNRP1: 41%, siGIPC1: 17%, siSyx: 1%, respectively**)**. When exogenous VEGF-A was added, it increased proliferation of si-Control-treated DJM-1 cells (white colums, siControl: 162%). However, exogenous VEGF-A did not induce the proliferation of siNRP1-, siGIPC1, or siSyx-treated cells (white columns, siNRP1: 60%, siGIPC1: 22%, siSyx: 13% respectively), suggesting that GIPC1 and Syx were downstream molecules responsible for the VEGF-A/NRP1 signal that induces proliferation of DJM-1 cells.

1-3-6. Syx RhoGEF activity was important for signaling DJM-1 cell proliferation.

MAPK and PI3K pathways are responsible for tumor malignancy and poor patient prognosis. The phosphorylation of MAPK (ERK) and Akt has been shown to contribute to cell proliferation and survival[44,45]. However, siVEGF-A and siNRP1 did not significantly change the phosphorylation levels of either MAPK or Akt in DJM-1 cells from those in siControl cells **(Fig. 1-6A)**. These results suggest that MAPK and Akt were not involved in the VEGF-A/NRP1-induced DJM-1 cell proliferation.

RhoA is a regulator of cell proliferation that drives the cell cycle into the S phase[35]. In siControl-treated cells, RhoA was activated in the absence of exogenous VEGF-A **(Fig. 1-6B**, 0 min, asterisk**)**. In contrast, the siVEGF-A-treatment inhibited the activation of

RhoA in the absence of exogenous VEGF-A **(Fig. 1-6B**, 0 min, asterisk**)**. The exogenous addition of VEGF-A activated RhoA in siControl-treated and siVEGF-A-treated cells **(Fig. 1-6B**, 5 min, 60 min**)**. All siNRP1-, siGIPC1, and siSyx-treatment abrogated RhoA activity in the absence of VEGF-A (-) **(Fig. 1-6C)**. The exogenous addition of VEGF-A (+) restored the RhoA activity of the siVEGF-A-treated cells, but not in siNRP1-, siGIPC1- and siSyx-treated DJM-1 cells **(Fig. 1-6C)**, indicating that the VEGF-A/NRP1 signal induced the activation of RhoA via GIPC1 and Syx in DJM-1 cells.

RhoGEF is an activator of RhoA. The Syx RhoGEF domain is located from 423 to 612 of its amino acid sequence[46] **(Fig. 1-6D)**. The amino acid residue Leu, located at 571, is important for the binding and activation of RhoA. In order to elucidate whether Syx RhoGEF activity was important for VEGF-A/NRP1-induced DJM-1 cancer cell proliferation, we constructed a lentivirus vector encoding Syx WT or Syx mutant with point mutation at the position of 571 Leu replaced to Glu in order to lose binding and the activation of RhoA[46]. The lentiviruses of Syx WT and the Syx mutant both induced protein expression in DJM-1 cells. The infection amounts among the viruses with the different titers for protein expression were adjusted for equal expression levels in the RhoA activity assay and colony formation assay **(Fig. 1-6E)**. The lentiviral overexpression of the Syx mutant protein interfered with the VEGF-A-induced activation of RhoA in DJM-1 cells **(Fig. 1-6F)** and inhibited DJM-1 cell proliferation (no addition: 100%, Syx WT: 129%, Syx MT: 45%) **(Fig. 1-6G)**. These results suggested that Syx, the RhoGEF of RhoA, was an essential and key signaling molecule for mediating VEGF-A-induced signal transduction that activates RhoA, leading to DJM-1 cell proliferation.

1-3-7. RhoA was activated by VEGF-A/NRP1, GIPC1 and Syx to promote cancer cell proliferation.

In order to determine whether the activation of RhoA promoted DJM-1 cell proliferation, DJM-1 cells were treated with C3 exoenzyme, a specific inhibitor of RhoA. C3 exoenzyme completely suppressed DJM-1 cell proliferation, both in the absence and the presence of exogenous VEGF-A (2% and 1% of siControl, respectively) **(Fig. 1-7A)**. Y27632, a ROCK inhibitor that is a downstream effector of RhoA, suppressed DJM-1 cell proliferation (no addition: 100%, 10 μM: 51%, 20 μM: 50% respectively) **(Fig. 1-7B)**. Proliferation was recovered (31% to 82%) when RhoA constitutively active form

(RhoA CA) was overexpressed in siVEGF-A-treated DJM-1 cells **(Fig. 1-7C,D)**. p27 was degraded by the activation of RhoA, thereby leading to cell proliferation (S-phase entry). p27 is an inhibitor of G1 cyclin dependent kinase and regulates cell proliferation downstream of RhoA. Under anchorage-independent conditions, the accumulation of p27 was greater in siVEGF-A- and siNRP1-treated DJM-1 cells than in siControl-treated DJM-1 cells **(Fig. 1-7E)**. Taken together, these results demonstrated that VEGF-A/NRP1 signaling activated RhoA activity via a GIPC1/Syx complex to inhibit the accumulation of p27.

1-3-8. The oligopeptide that inhibited GIPC1 and Syx interactions suppressed RhoA activation and DJM-1 proliferation.

We designed a membrane-penetrating peptide targeted to inhibit complex formation between GIPC1 and Syx **(Fig. 1-8A)**. The 30 kDa Targeted peptide consisted of TAT, a cell penetrating sequence of the HIV virus, EGFP, and eight amino acid residues that included the Syx C terminal amino acid sequence (STLTASEV). The Syx C-termial amino acid sequence was important for recognizing the GIPC1 PDZ domain in the GIPC1/Syx interaction; therefore, the Targeted peptide acted as a competitive inhibitor. The incorporation of these peptides into DJM-1 cells was confirmed through the detection of a green fluorescent protein linked to the peptide after 1 h treatment **(Fig. 1-8B)**. In order to establish whether the Targeted peptide interacted with GIPC1, HA-tagged GIPC1 was overexpressed in HEK293T cells and the cell lysate was incubated with either the Scrambled peptide or Targeted peptide. Binding of the Targeted peptide with GIPC1 was 3- fold greater than that with the Scrambled peptide **(Fig. 1-8C)**. In order to evaluate whether the Targeted peptide inhibited the interaction between GIPC1 and Syx, NRP1, GIPC1, and Syx vectors were transfected and expressed in HEK293T cells and these cells were then treated with the Targeted or Scrambled peptide for 16 h. After a 10 min stimulation with (+) or without (-) VEGF-A (100 ng/ml), the cells were lysed and the indicated proteins in the cell lysates were co-immunoprecipitated with V5-tagged Syx (left panels). VEGF-A/NRP1 induced GIPC1/Syx complex formation in the presence of the Scrambled peptide **(Fig. 1-8D, asterisk)**. On the other hand, the Targeted peptide abrogated the VEGF-A/NRP1 signal-induced GIPC1/Syx interaction **(Fig. 1-8D, asterisk)**. In addition, the Targeted peptide more strongly prevented the activation of RhoA than the Scrambled peptide in the

absence and presence of VEGF-A **(Fig. 1-8E)**. Additionally, DJM-1 cell proliferation was inhibited by the Targeted peptide (Scramble peptide: 99%, Targeted peptide: 43%) **(Fig. 1-8F)**. These results demonstrated that, in the VEGF-A/NRP1 signaling pathway, the GIPC1 and Syx interaction was necessary the activation of RhoA in order to promote the proliferation of cancer cells.

1-4. Figures and Legends

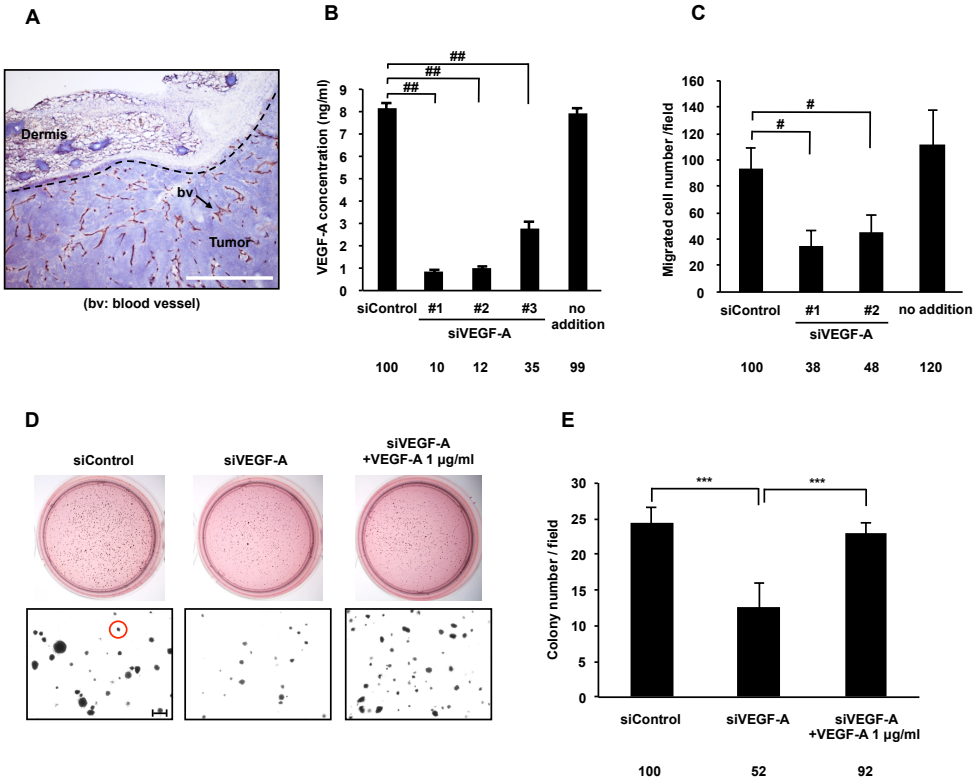

Fig. 1-1. VEGF-A secreted by DJM-1 cells induced tumor angiogenesis and cancer cell proliferation.

(A) Frozen sectioned DJM-1 tumors were stained with the endothelial marker CD-31 and hematoxylin. The arrow indicates blood vessels (Scale bar: 100 μm). (B) Quantification of VEGF-A concentrations secreted by DJM-1 cells. After a 72 h treatment with (20 nM, siControl, or siVEGF-A #1–3) or without siRNA (no addition), conditioned media were collected and analyzed by VEGF-A ELISA. (C) HUVEC migration assay. (B,C) Data represent the means±s.d. Percentages from the each mean relative to siControl are indicated below the graph. (D) Endogenous VEGF-A induced colony formation by cancer cells. DJM-1 cells were treated with siControl or siVEGF-A #1 (20 nM each) and seeded in soft agar. The upper panel shows the bright field of MTT staining colonies; the lower panel shows magnified colonies (Red circle: >80 μm diameter, Scale bar: 250 μm). (E) Quantitative analysis of D. The means of colony numbers in 6 fields for each condition are shown with ±s.d. Percentages from each mean relative to the siControl are indicated below the graph. $^{\#}P<0.05$; $^{\#\#}P<0.01$; **P<0.005; ***P<0.001.

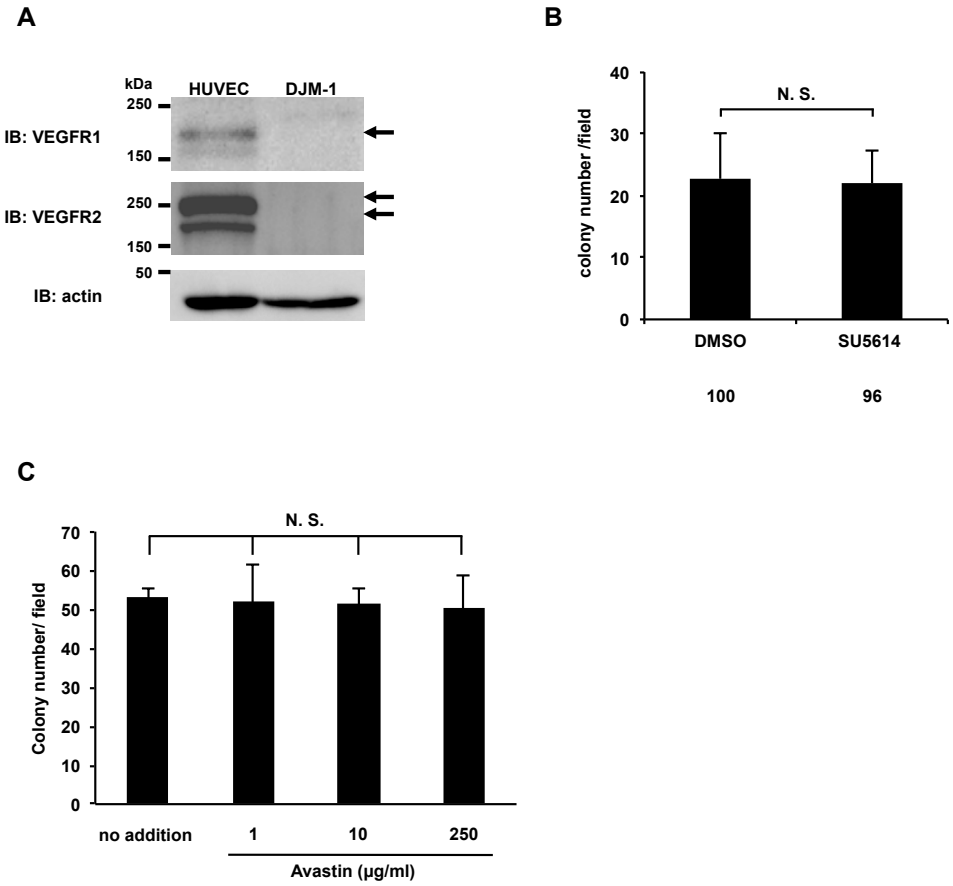

Fig. 1-2. The VEGFR kinase inhibitor SU5614 and Avastin did not inhibit DJM-1 cell proliferation.

(A) Western blot for VEGFR1 or VEGFR2 of DJM-1 cell lysates. As a positive control, the cell lysates of HUVEC were applied in the left lanes. Arrows indicate VEGFR1 or VEGFR2. (B) Colony formation assay for DJM-1 cells treated with 10 μM SU5614, the VEGFR kinase inhibitor, and with 0.2% DMSO as the control. (C) DJM-1 cell colony formation assay treated with Avastin (from 1 to 250 μg/ml). These data represent the means±s.d. N.S., not significant. Percentages from each mean relative to the DMSO (B) or no addtion (C) are shown below the graph.

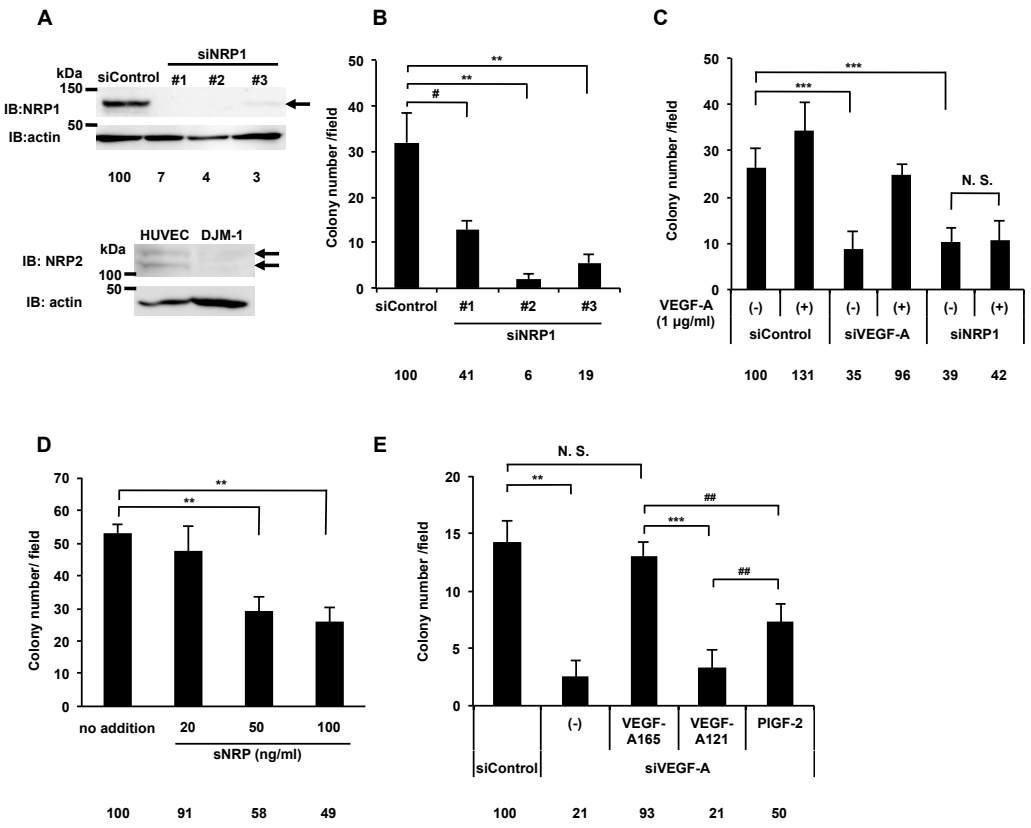

Fig. 1-3. VEGF-A promoted DJM-1 cell proliferation via NRP1 in an autocrine manner. (A) A western blot shows that DJM-1 cells expressed NRP1, but not NRP2. DJM-1 cells were treated with siRNA (siControl, siNRP1 #1–3, 20 nM each) for immunoblotting the NRP1 protein (arrow indicates NRP1; 130 kDa). Percentages from each blotted protein amount relative to the siControl are indicated below each lane. Actin was immunoblotted to normalize the amounts of NRP1 (upper panel). HUVEC expressed NRP2, whereas DJM-1 cells did not (arrows indicate NRP2; 120–130 kDa, lower panel). (B) DJM-1 cell colony formation assay. Cells treated with 20 nM siControl and siNRP1 #1–3. (C) Colony formation by siVEGF-A- or siNRP1-treated DJM-1 cells. The presence or absence of exogenous VEGF-A (1 μg/ml) was indicated as (+) and (-) respectively. (D) DJM-1 cell colony formation assay in the presence of sNRP (from 20 to 100 ng/ml). (E) The graph shows the effects of VEGF-A family members (1 μg/ml each) in the siVEGF-A-treated DJM-1 cell colony formation assay. These data represent the means±s.d. Percentages from each mean relative to the siControl (B,C,E) or no addition (D) are shown below the graph. N.S., not significant; $^{\#}P<0.05$; $^{\#\#}P<0.01$; **P<0.005; ***P<0.001.

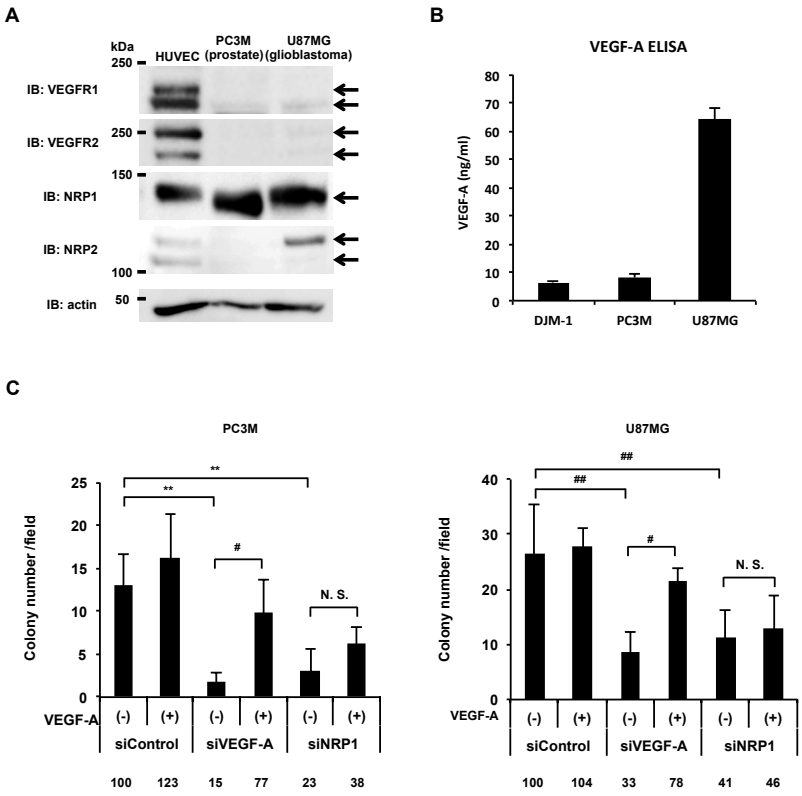

Fig 1-4. VEGF-A/NRP1 signaling pathway promoted PC3M and U87MG cell proliferation.

(A) Western blot shows that VEGFR1, VEGFR2, NRP1 and NRP2 expression in prostate cancer, PC3M and glioblastoma, U87MG cells. HUVEC in the left lane, as a positive control for the receptors. Arrows indicate VEGFR1, VEGFR2, NRP1 or NRP2. (B) Quantification of VEGF-A concentration secreted by DJM-1, PC3M, and U87MG cells. After 72 h culture, the conditioned media were collected and analyzed by VEGF-A ELISA. Measurement of VEGF-A concentration from the each sample was duplicated and the ELISA experiment was repeated twice. These data represent the means ± S.D. (C) Evaluation of endogenous VEGF-A/NRP1 signal-induced proliferation of PC3M and U87MG cells in an anchorage-independent condition. The cells were treated with siControl, siVEGF-A or siNRP1 (20 nM each). The presence or absence of VEGF-A (1 μg/ml) were indicated as (+) or (-) respectively. The means of colony numbers in 7 fields for each condition are shown with ± S.D. The percentages from the each mean compared to siControl (-) are indicated below the graph. N.S., not significant; #P<0.05; ##P<0.01; **P<0.005; ***P<0.001.

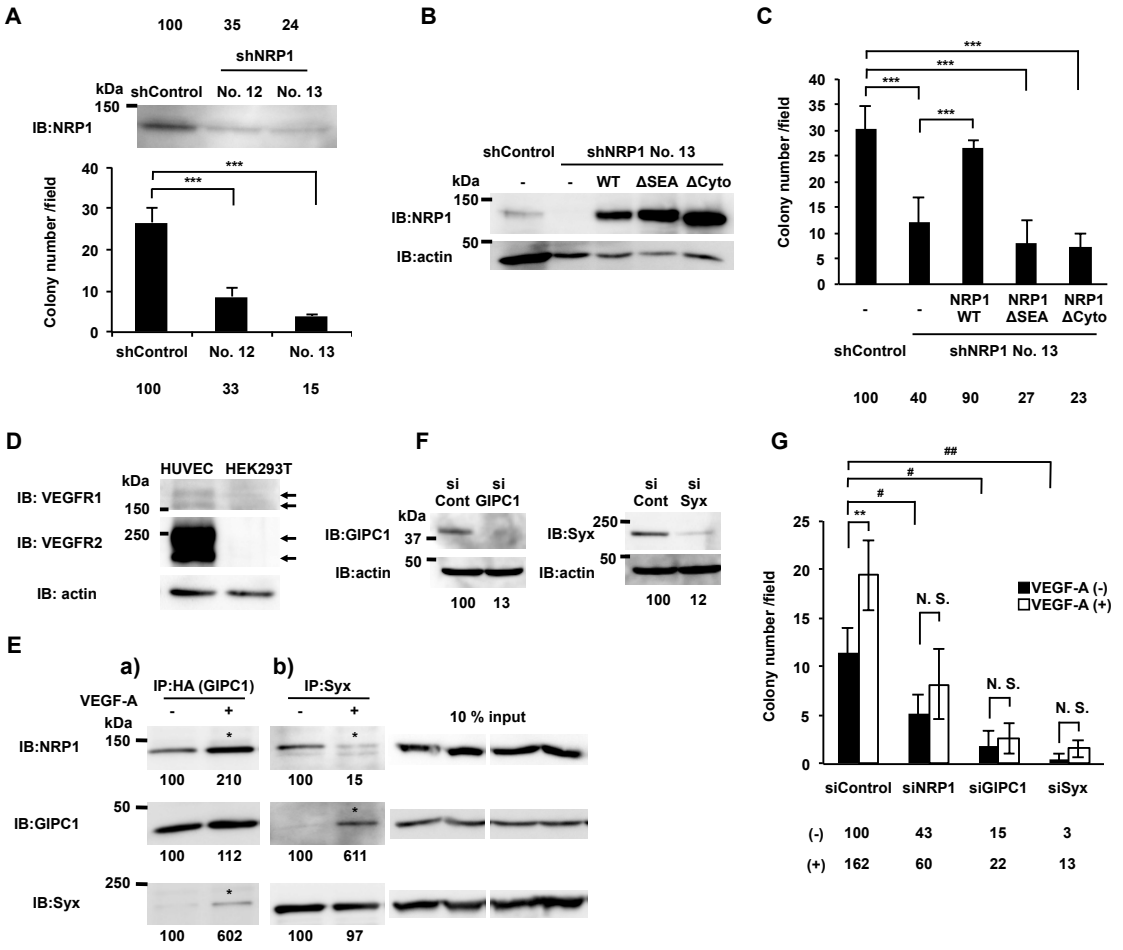

Fig. 1-5. The NRP1 cytoplasmic region was essential for VEGF-A-induced cancer cell proliferation.

(A) The western blot shows the expression of NRP1 in shControl- or NRP1 shRNA-treated DJM-1 clones (No. 12 and No. 13). NRP1 expression was normalized by each actin to compare inhibitory efficiency of shNRP1 clone. Percentages from each mean relative to the siControl are shown besides the graph. (B) The comparison of NRP1 expression levels among lentivirus-overexpressed NRP1WT or cytoplasmic region deletion mutants (NRP1ΔSEA or NRP1ΔCyto) in shNRP1 DJM-1 No.13 clone (upper lanes). The same proteins were re-immunoblotted with an anti-actin antibody (lower lanes). (C) The colony formation assay of the lentivirus-overexpressed NRP1WT, NRP1ΔSEA or NRP1ΔCyto in the shNRP1 DJM-1 No.13 clone and shControl DJM-1 clone. (A,C) Percentages from each mean relative to the shControl are shown below the graph. (D) Western blot shows VEGFR1 and VEGFR2 expression in HEK293T cells. HUVEC as a loading control (left lane). Arrows indicateVEGFR1 or VEGFR2. (E)

Co-immunoprecipitation assay with GIPC1 (a) or Syx (b). NRP1, GIPC1, and Syx were expressed in HEK293T cells and treated without (-) or with (+) VEGF-A (100 ng/ml) for 15 min. (a) Increased NRP1/GIPC1 and GIPC1/Syx interactions in the presence of VEGF-A are indicated by asterisks. (b) The Syx/GIPC1 interaction was increased in the presence of VEGF-A (asterisk). On the other hand, the NRP1/Syx interaction was decreased (asterisk). A 10% input as the loading control of NRP1, GIPC1, and Syx co-expressed in HEK293T cell lysates are shown in the right panels. Percentages from each blotted protein amount relative to "VEGF-A (-)" are shown below each lane. (F) Confirmation of the siRNA effects for GIPC1 or Syx. GIPC1 or Syx was overexpressed in HEK293T cells treated with 20 nM siControl, siGIPC1, or siSyx. The inhibitory efficiency of each siRNA on the expression of GIPC1 or Syx that normalized each actin was compared to the siControl. The inhibitory percentages relative to the siControl are shown below each lane. (G) Colony formation assay in siNRP1, siGIPC1, or siSyx treated-DJM-1 cells in the presence or absence of exogenous VEGF-A (1 μg/ml) indicated as white columns (+) or black columns (-), respectively. Percentages from each mean relative to the siControl are shown below the graph. These data represent the means±s.d. N.S., not significant; $^{\#}$P<0.05; $^{\#\#}$<P0.01; **P<0.005; ***P<0.001.

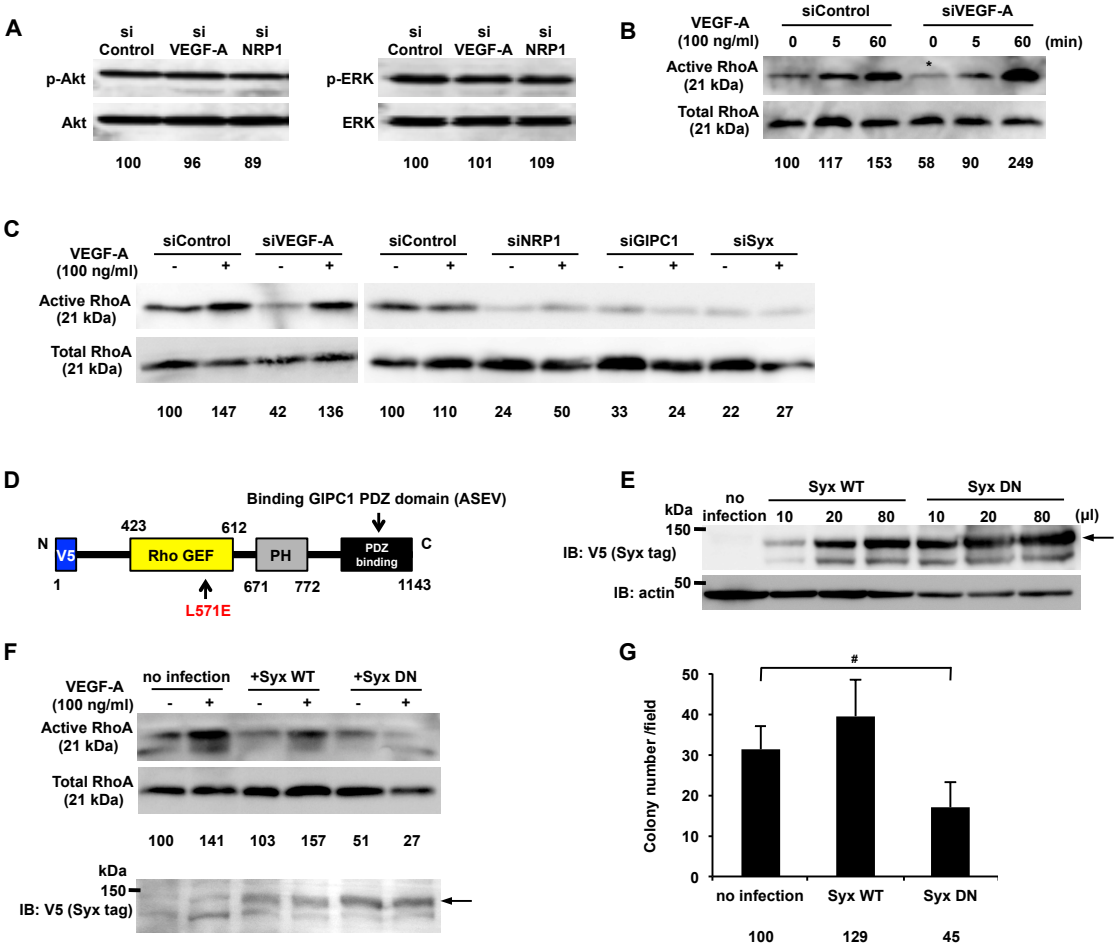

Fig. 1-6. Syx was identified as a downstream molecule of VEGF-A/NRP1 signaling and a RhoA activator that promoted DJM-1 cell proliferation.

(A) The western blot for phospho-Akt and phospho-ERK of DJM-1 cell lysates. DJM-1 cells were treated with siRNAs (siControl, siVEGF-A or siNRP1, 20 nM respectively) under anchorage-independent conditions. The same proteins were re-immunoblotted with an anti-Akt or -ERK antibody to normalize the amounts of each phospho-protein. (B,C) The RhoA activity of DJM-1 cells under anchorage-independent conditions. (B) DJM-1 cells were treated with siControl or siVEGF-A and stimulated with (+) or without (-) VEGF-A (100 ng/ml) at the indicated time points. The siVEGF-A treatment (asterisk) decreased RhoA activity below that with the siControl treatment. (C) DJM-1 cells were treated with siVEGF-A, siNRP1, siGIPC1, and siSyx in the presence of VEGF-A (+) or its absence (-). (D) Structure of dominant negative Syx (Syx DN). An amino acid substitution of Leu 571 Glu in Syx DN prevented RhoA from interacting with the mutant. The V5 epitope was tagged at the N-terminus of Syx DN. (E) Lentiviral

overexpression of Syx WT or Syx DN in DJM-1 cells. Virus infection amounts were adjusted for equal expression levels of Syx WT or Syx DN in the RhoA activity assay (F) and in the colony formation assay (G). Arrow shows Syx WT or Syx DN. (F) The RhoA activity assay for Syx DN-overexpressing DJM-1 cells under anchorage-independent conditions in the presence of VEGF-A (100 ng/ml) (+) or its absence (-). A 10% input was subsequently immunoblotted with an anti-V5 antibody to normalize the amounts of each protein. The arrow shows Syx WT or Syx DN. (G) The colony formation assay for DJM-1 cells that overexpressed Syx WT or Syx DN. These data represent the means±s.d. Percentages from each mean relative to the siControl (A), siControl (-) (B,C) or no infection (F,G) are shown below the graph. $^{\#}P<0.05$.

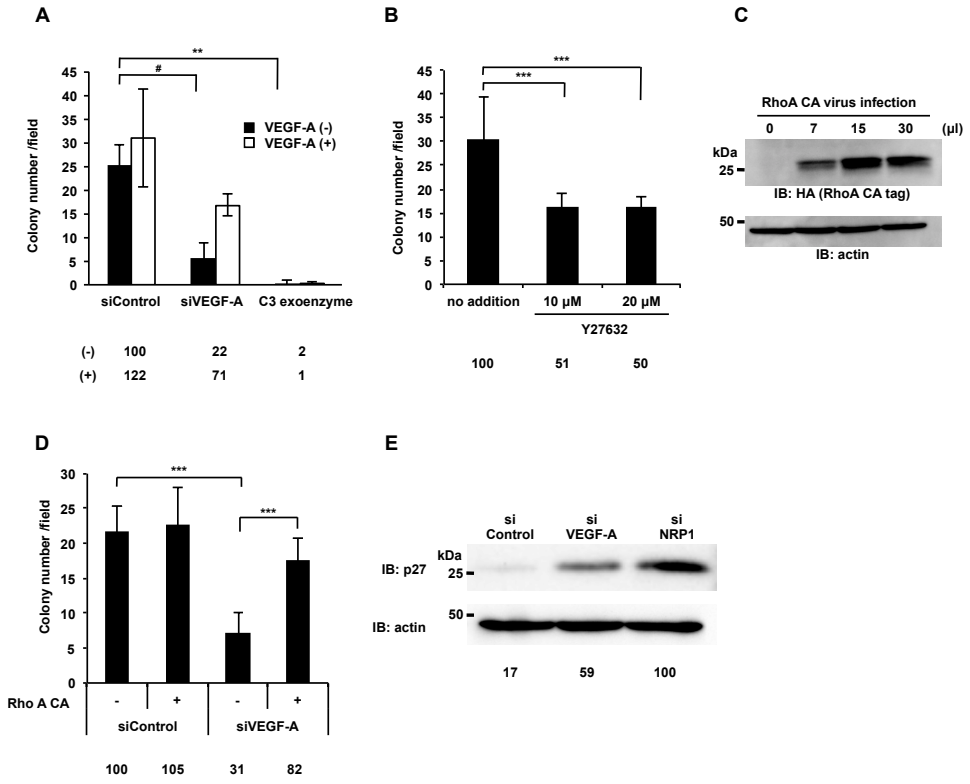

Fig. 1-7. RhoA activity was essential for the DJM-1 cell proliferation signal to induce p27kip1 protein degradation.

(A,B) The colony formation assay for DJM-1 cells. (A) DJM-1 cells were treated with siRNAs (siControl, siVEGF-A, 20 nM each) and C3 exoenzyme (2 μg/ml) in the presence or absence of exogenous VEGF-A (1 μg/ml), indicated as white columns (+) or black columns (-), respectively. (B) DJM-1 cells were treated with the ROCK inhibitor, Y27632 (10 or 20 μM). (C) An increase in the lentiviral infection of RhoA constitutively active form (RhoA CA) enhanced the RhoA active form in DJM-1 cells. (D) The colony formation assay for siRNAs (siControl or siVEGF-A, 20 nM each) treated-DJM-1 cells with (+) or without (-) RhoA CA expression. Percentages from each relative to the siControl (-) (A,D) or no addition (B) are shown below the graph. (E) DJM-1 cells were treated with siControl, siVEGF-A, or siNRP1 (20 nM each) under anchorage-independent conditions and total cell lysates were immunoblotted with an anti-p27 antibody. Percentages from the p27 level in each siRNA treated-cell lysate relative to siNRP1 are indicated below the lane. The same proteins were re-immunoblotted with an anti-actin antibody to normalize the amounts of each protein. These data represent the means±s.d. $^{\#}P<0.05$; $^{**}P<0.005$; $^{***}P<0.001$.

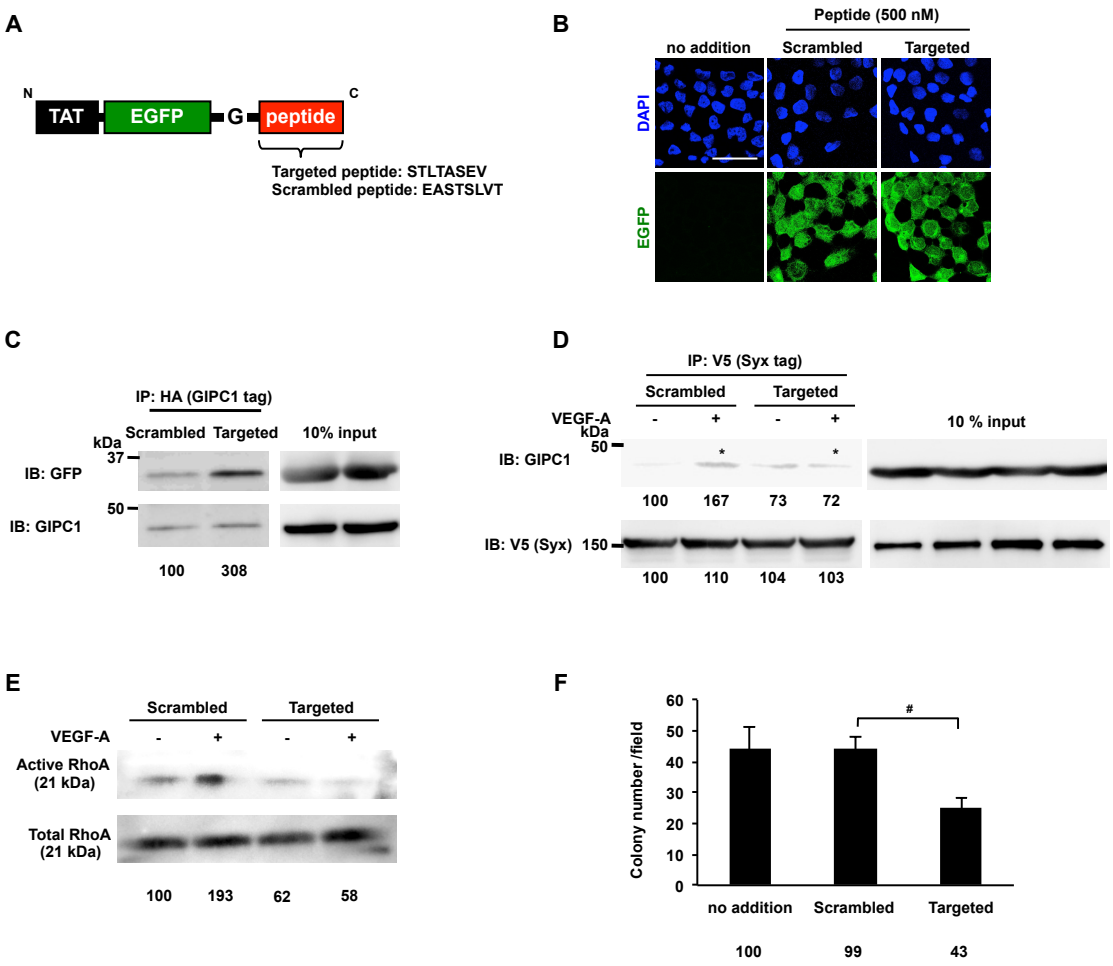

Fig. 1-8. The oligopeptide that inhibited the GIPC1 and Syx interaction suppressed RhoA activity and the proliferation of DJM-1 cells.

(A) A schematic of the construct that contained TAT, EGFP, and the Gly insertion prior to the Targeted peptide sequence (STLTASEV; Syx C terminus sequence). The Scrambled peptide amino acid sequence is also shown in the lower case (EASTSLVT). (B) Confirmation of the peptide incorporation into DJM-1 cells. DJM-1 cells were treated with the Scrambled or Targeted peptide (500 nM each) for 1 h. Confocal images indicated the Scrambled or Targeted peptide in the intracellular region of DJM-1 cells (green). Nuclei in the same position were shown in the upper panels (blue). Scale bar: 30 μm. (C) The co-immunoprecipitation assay with the Target peptide. HA-tagged GIPC1 was overexpressed in HEK293T cells. The Scrambled or Targeted peptide was mixed with the cell lysate and co-immunoprecipitated with GIPC1 after a 1 h rotation at 4°C. The same lysates (10% input) were immunoblotted with anti-GFP or

anti-GIPC1 antibodies to normalize the amounts of the peptide and GIPC1. Percentages from each relative to the Scrambled are shown below the graph. (D) NRP1, GIPC1, and Syx vectors were transfected and expressed in HEK293T cells, which were subsequently treated with the Targeted or Scrambled peptide for 16 h. After a 10 min stimulation with (+) or without (-) VEGF-A (100 ng/ml), the cells were lysed and the indicated proteins in the cell lysates were co-immunoprecipitated with V5- tagged Syx (left panels). VEGF-A induced the GIPC1/Syx interaction in the presence of the Scrambled peptide (asterisk). On the other hand, the Targeted peptide abrogated the GIPC1/Syx interaction (asterisk). Percentages from each protein level [GIPC1 or V5 (Syx)] compared to the lane of Scrambled (-) are indicated below the lane. The same lysates (10% input) were immunoblotted with anti-GIPC1 or V5 antibodies to normalize the amounts of each protein. (E) The RhoA activity assay. DJM-1 cells were treated with the Targeted or Scrambled peptide and stimulated with (+) or without (-) VEGF-A (100 ng/ml) under anchorage- independent conditions. The same lysates (10% input) were immunoblotted with an anti-RhoA antibody to normalize the protein amounts with each treatment. Percentages from each relative to the Scrambled (-) are shown below the graph. (F) The colony formation assay. DJM-1 cells were treated with 500 nM of the Targeted or Scrambled peptide. The Targeted peptide inhibited DJM-1 cell proliferation, whereas the Scrambled peptide did not. These data represent the means±s.d. Percentages from each mean relative to the no addition control are shown below the graph. $^{\#}P<0.05$.

1-5. Discussion

In the present study, VEGF-A induced the cancer cell proliferation of PC3M (prostate cancer), DJM-1 (skin cancer), and U87MG (glioblastoma) in an anchorage-independent manner via the NRP1 signaling pathway. The knockdown of VEGF-A or NRP1 abrogated the proliferation of these cancer cells. We selected skin cancer-derived DJM-1 cells, which only express NRP1 as the VEGF-A receptor and grow faster than other cancer cells under anchorage-independent conditions. In cancer cells, VEGF-A did not show strong effects in anchorage-dependent growth, however, VEGF-A conferred proliferative activity in anchorage-independent conditions (data not shown). In cancer cells, the ability to exhibit anchorage-independent cell growth, has been connected with tumor cell aggressiveness in vivo such as tumorigenic and metastatic potentials[47].

The NRP1 structure governs its bioactivity. The treatment of cancer cells with soluble NRP1 B domain or siNRP1 inhibited proliferation in an anchorage-independent manner. Stable shNRP1-DJM-1 clones also decreased the proliferation. Together, these results indicate that endogenous NRP1 transduced a VEGF-A proliferative signal. PlGF, a member of VEGF-A family, activated MAPK pathway via NRP1 in medulloblastoma[11]. NRP2, an isoform of NRP1, was previously shown to transduce the activation of AKT in pancreatic cancer cells[48]. However, in the present study, these pathways were not involved in VEGF-A/NRP1 signaling because ERK and Akt phosphorylation levels did not change even when the expression of VEGF-A or NRP1 was decreased by siRNA. The NRP1 C-terminal 3 amino acids (SEA), which contribute to recognition of the PDZ domain of GIPC1, were of particular interest in the present study. The SEA motif was previously shown to be critical for binding GIPC1[18]. In the present study, lentiviral infection of the two NRP1 cytoplasmic deletion mutants (NRP1ΔSEA or NRP1ΔCyto) into the shNRP-DJM1 clone failed to induce anchorage-independent growth in response to VEGF-A. VEGF-A increased GIPC1 interaction with NRP1, indicating that NRP1/GIPC1 interaction is necessary for stimulating DJM-1 cell proliferation. GIPC1 has been suggested to play an important role in cancer cell proliferation. GIPC1 was shown to bind to IGF-1R via its PDZ domain in order to promote pancreatic cancer cell proliferation[24]. By binding VEGF-A to NRP1, GIPC1 mediates the interaction between NRP1 and ABL1, which activates tyrosine kinase activity and associates with integrins, leading to induce tumor growth[49]. Syx is a RhoGEF that stimulates RhoA activity[29]. The

molecular interaction between GIPC1 and Syx has been identified by two-yeast hybridization[28]. Although Syx has not reported to have a NRP1 binding cite, in the present study, Syx seemed to interact with NRP1 in the absence of VEGF-A. So far, only GIPC1 has been reported to have the ability to bind the cytoplasmic region of NRP1, but recently, using anti bait co-immunoprecipitation and mass-spectroscopy analysis Seerapu et al. demonstrated that Filamin-A (FlnA), which does not have a PDZ domain, could directly bind NRP1 cytoplasmic region[50]. This study did not reveal how NRP1 interacts with Syx in VEGF-A stimulated cells, it should be elucidated which amino acid sequences are important for binding Syx and NRP1. Syx has been implicated in tumorigenesis, in brain tumors and in neuroblastoma[31]. siSyx inhibited the proliferation of DJM-1 cells, indicating that Syx involved in a signaling pathway that promotes cancer cell proliferation.

RhoA is a small GTPase that drives the cell cycle into the S-phase with degradation of p27. A majority of human malignancies in many organ sites show reduced p27 protein levels[35]. Activation of RhoA induces protein degradation of $p27^{Kip1}$. The "dominant negative" effect of the Syx mutant (SyxDN) on RhoA suggests that Syx is in the VEGF-A/NRP1 signaling pathway. RhoA has been implicated in virtually all stages of cancer progression. Treatment of DJM-1 cells with the RhoA specific inhibitor, C3 exoenzyme, or ROCK inhibitor (Y27632) suppressed DJM-1 cell proliferation. Knockdown of VEGF-A or NRP1 upregulated p27 protein. In addition, overexpression of constitutively active RhoA in siVEGF-A-treated cells rescued the inhibition of proliferation, indicating that endogenous VEGF-A-binding NRP1 causes activation of Syx RhoGEF to stimulate RhoA activation, leading to p27 degradation. Together, these results suggest that endogenous VEGF-A/NRP1 signaling in DJM-1 cells induces p27 degradation to constitutively stimulate progress into the S-phase.

An importance of the molecular mechanism by which GIPC1 interaction with Syx activates Syx GEF activity was demonstrated in this study. A recent report has shown that MyoGEF, another activator of RhoGTPase, has the similarity in the C-terminus of three amino acids SEV that interacts with GIPC1 to promote breast cancer cell invasion[26]. The SEV amino acids are also located in the C-terminus of Syx. In this study, as a novel tactics, we generated a peptide that contains HIV TAT sequence which enables the peptide to penetrate cell membrane and that inhibits the complex formation of GIPC1 and Syx. The peptide consists of eight amino acids corresponding

to the sequence of Syx C-terminus (STLTASEV). C-terminal five or six amino acids of a binding partner of GIPC1 give rise to the enough affinity to bind for the PDZ domain[24]. This study showed that the peptide abrogated the complex forming that is necessary for Syx RhoGEF activation. It has been reported that Syx includes an auto-inhibitory domain in the C-terminal region. It is a hypothetical mechanism by which GIPC1 binding to the auto-inhibitory domain in the C-terminal region of Syx triggers the RhoGEF activity[46].

In conclusion, this study provides evidence for a new pathway of VEGF-A/NRP1 signaling leading to proliferation in cancer cells. Furthermore, it shows that the molecular function of GIPC1 and its interaction with Syx plays a key role for RhoA activation, which induces p27 degradation. We believe that the inhibition of VEGF-A/NRP1 signaling could provide a new strategy against cancer and could be applied in the design of new cancer drugs.

Chapter 2.

VEGF-A/Neuropilin-1 signaling activates RhoA and promotes cancer cell invasiveness and metastasis.

2-1. Introduction

Cancer invasiveness is one of the most important processes of cancer progression. Neuropilin-1 (NRP1) is a multifunctional protein frequently expressed in cancer cells and has been linked to tumor progression and metastasis[11,51].

NRP1 is 130 kDa of single-transmembrane glycoprotein identified as VEGF-A receptor, which is an essential for angiogenesis and is expressed in both endothelial cells and cancer cells[6]. In endothelial cells, NRP1 enhanced VEGFR2 signaling by promoting a complex formation between the VEGF-A, VEGFR2 and NRP1 molecules[52]. In cancer cells, the extracellular domain of NRP1 functioned as a reservoir for VEGF-A enrichment in the peritumoral area to recruit blood vessels into the tumor[52]. Blockade of NRP1 inhibited VEGF-A-induced angiogenesis and tumor growth[53]. Additionally, high expression of VEGF-A in melanoma cells expressing NRP2, an isoform of NRP1, was increased tumor angiogenesis and metastasis to the lung and lymph nodes[54].

Thus, cancer cell-secreted VEGF-A has a key role in blood vessel growth, especially in tumor angiogenesis followed by metastasis[3]. Although most studies on VEGF-A and NRP1 have been focused on their function in angiogenesis and in endothelial cells, the role of VEGF and VEGF-A/NRP1 signaling in cancer cells is an emerging area of importance.

In Chapter 1, I showed that NRP1 expressed in several cancer cells, such as human skin cancer, glioblastoma and prostate cancer cells, transducing a proliferative signal

from VEGF-A in an autocrine manner. In detail, the VEGF-A signal induced the formation of NRP1/GIPC1 and GIPC1/Syx complexes and promoted the activation of RhoA activity.

GIPC1, a PDZ adaptor protein, interacts with the end of C-terminus of NRP1 containing SEA[18]. In cancer cells, the function of GIPC1 has been reported to be a binding for different molecules, like IGF1R, TGFR to promote cancer growth[24]. Syx is a RhoGEF, which was identified as a binding partner of GIPC1 by two-yeast hybridization[28]. Syx is expressed in several types of cancers, such as neuroblastoma, other brain tumors, and breast cancer[30,55]. I showed that VEGF-A stimulated activation of Syx-RhoGEF activity by induces binding to GIPC1 with Syx and leading to RhoA activation[56]. RhoA has been shown to be a regulator of cell proliferation in different types of cancer cells[35]. Overexpression of RhoA increased cancer cell malignancies. There have been reports that RhoA functions as a regulator of motility and invasiveness in many types of cancer cells. The RhoA expression level correlates with cancer cell invasiveness. RhoA enhanced invasiveness of hepatocellular carcinoma[13] and bladder cancer[57], and also promoted the progression of esophageal squamous carcinoma, gastric cancer, colon, lung and ovarian cancer[58-61].

Syx has SEV amino acids that interact with the GIPC1 PDZ domain in its C-terminal[30]. To inhibit GIPC1 and Syx interaction, cancer cells were treated with a peptide that containing HIV-TAT sequence which enabled the peptide to penetrate the cell membrane, and eight amino acids corresponding to the sequence of Syx C-terminus (STLTASEV). The peptide inhibited the complex formation of GIPC1 and Syx by abrogated VEGF-A/NRP1-induced RhoA activation and cancer cell proliferation.

In chapter 2, the VEGF-A/NRP1 signaling leading to RhoA activation promoted cancer cell invasion in skin, prostate and glioblastoma cells and increased skin cancer metastasis to lymph node in mouse models. The targeting Syx C-terminal peptide diminished cancer invasion followed by VEGF-A-induced RhoA activation. The cytoplasmic deletion mutants of NRP1-expressed skin tumors showed reduction of growth and significantly suppressed metastasis to lymph nodes. For VEGF-A autocrine signaling, the NRP1 cytoplasmic region is essential for GIPC1 interaction with Syx, which is a key event in activation of RhoA activativity, resulting in cancer invasion and metastasis.

2-2. Materials and Methods

2-1-1. Animal studies

All animal experiments were performed in accordance with Kyoto Sangyo University's animal experiment guidelines. Tumor xenografts were established from intradermal injections of DJM-1 cells (4×10^6 cells per 100 μl HBSS, GIBCO; Life Technologies) into the right flank of 8-week female BALB/C Slc-nu/nu mice (SHIMIZU Laboratory Supplies Co., Ltd, Kyoto, Japan). The isolated tumors and lymph nodes from the sacrificed mice were embedded in OCT compound (SAKURA Tissue Teck, Tokyo, Japan) for immunohistochemistry.

2-2-2. Cell culture and transfection

DJM-1 cells were cultured as in chapter 1[62]. Human prostate cancer, PC3M cells and Human Glioblastoma, U87MG cells were purchased from ATCC. PC3M cells were cultured in RPMI-1640 supplemented with 10% fetal bovine serum (FBS) (GE Healthcare, Little Chalfont, UK), 2 mmol/L L-glutamine, 50 U/mL penicillin and 50 μg/mL streptomycin. U87MG cells were cultured in EMEM supplemented with 10% FBS.

Stable shRNA transfection into DJM-1 cells was performed by electroporation as described previously[56]. SiLentFect™ reagents (Bio Rad) were used for all siRNA treatments, as directed in the manufacturer's instructions. 5 μg/ml polybrane (Millipore) was used for virus infection. Cells were seeded in 5 mg/ml polyHEMA (poly 2-hydroxyethyl methacrylate) (SIGMA, St. Louis, Missouri MO, USA)-coated 100 mm dishes to culture under anchorage-independent conditions[40].

2-2-3. Antibodies

Anti-neuropilin-1 (D62C6) and RhoA (67B9) antibodies were purchased from Cell Signaling Technology (Danvers, Massachusetts, USA). Flt-1 (VEGFR1) (C-17) rabbit, Flk-1 (VEGFR2) (C-1158) rabbit and Neuropilin-2 (C-9) mouse antibodies were purchased from Santa Cruz (Dallas, Texas, USA). Anti-actin mouse antibody was purchased from SIGMA. Anti-mouse CD31 (PECAM-1) (MEC 13.3) antibody was purchased from BD Biosciences Pharmingen (Franklin Lakes, New Jersey, USA). Anti-Keratin 14 antibody was purchased from NeoMarkers (Fremont, California, USA). Anti-Ki67 (MIB-1) mouse antibody was purchased from DAKO (Agilent Technologies, Santa Clara, CA, USA). Anti-GST hamster antibody was purchased from santacruz

(Dallas, Texas, USA). Anti-rabbit IgG horseradish peroxidase-conjugated was purchased from Jackson Immuno Research (West Grove, Pennsylvania, USA). Alexa-Fluor® 488 anti-rabbit IgG, 594 streptavidin and 4',6-diamidino-2-phenylindole were purchased from Life Technologies (Carlsbad, California, USA).

2-2-4. siRNAs

Control siRNA, was purchased from Dharmacon RNAi Technologies (Thermo Scientific, Waltham, Massachusetts, USA). The sequence of VEGF-A siRNA and NRP1 siRNA were described in chapter 1, and GIPC1 siRNA and Syx siRNA were listed in Table. 2-1.

2-2-5. Peptides

The cDNAs to encode oligopeptide sequences for Targeted peptide (STLTASEV: Targeted) and Scrambled peptide (EASTSLVT: Scrambled) were prepared by site-directed mutagenesis kit (GE Healthcare Life Sciences, Buckinghamshire, UK) as described in chapter 1. Incorporated images of the peptides in cancer cells were confirmed by confocal microscopy (x63, LEICA CTR 5500, Leica Camera AG, Leitz Park Wetzla, Germany).

2-2-6. Western Blotting

The Cells were washed with PBS and lysed with RIPA buffer (1% NP-40, 0.5% Sodium Deoxycholate, 0.1% SDS, NaCl 100 mM, Tris-HCl 50 mM, pH7.4). Samples were denatured with SDS-sample buffer and loaded into SDS-polyacrylamide gels. Proteins were transferred to a PVDF membrane (Millipore), and the membrane was blocked with 4% skim milk in TBST for 30 min. The membrane was incubated with primary antibody-diluted 4% skim milk in TBST at 4°C overnight. After the incubation, the membrane was washed with TBST and incubated with the appropriate HRP-conjugated secondary antibody at room temperature for 1 h. Detection was performed with SuperSignal® West Pico Chemiluminescent Substrate (Thermo Scientific) and chemiluminescence was measured by LAS-4000 mini (GE Healthcare, Piscataway, New Jersey, USA). Percentages from each band on densitometry compared to the control were indicated in the lower lanes in the figures. The western blot analysis was repeated 3 times.

2-2-7. VEGF-A ELISA

Human VEGF Quantikine® ELISA kit (R & D Systems) was used to measure VEGF-A levels in conditioned media. Cancer cells were seeded at the density of $8x10^5$ cells /35 mm dish. The medium was changed to basal medium containing 1% BSA, and cells

were incubated for 72 h. The conditioned media were diluted to one hundred-fold with serum free-DMEM, and VEGF-A levels were measured using the manufacturer's protocol.

2-2-8. RT-PCR

Cancer cells were treated with 20 nM siRNA and cultured for 72 h. Total RNA was isolated by ISOGEN II (NIPPON GENE Co., LTD., Toyama, Japan) as following manufacture protocol. Three-μg of total RNA from siRNA-treated cancer cells were reverse transcript to cDNA using the SuperScript First-Strand Synthesis System (Invitrogen). The following primers were used. NRP1 forward: 5'-GCTCCCGCCTGAACTA CCCTG-3', NRP1 reverse: 5'-GCCTTGCGCTTGCTGTCATC-3', GIPC1 forward: 5'-GCCTCGT GTTCCACACCCA-3', GIPC1 reverse: 5'-CAGATCGGGCTGGAGGACT-3', Syx forward: 5'-CTGGGCAAAGTGGACATCTA-3', Syx reverse: 5'-CATCCTCGTCTTCATCGTACTC-3', GAPDH forward: 5'-ACCACAGTCCATGCCATCAC-3', GAPDH reverse: 5'-TCCACCACCCTGTTGCTGT A-3'.

2-2-9. Colony formation assay

Cancer cells were treated with 20 nM siRNA or peptides before being seeded in agar. Two ml of growth medium containing 0.72% agar was prepared in a 35 mm dish and solidified as bottom agar. The cells (5×10^4 ~ 1×10^5 cells) were suspended in 2 ml culture medium containing 0.36% agar and, after the addition of ligands or chemicals, layered on the bottom agar. Viable cells were stained with 300 μg/ml 3-(4,5-Dimethyl-2-thiazolyl)- 2,5-diphenyl-2H-tetrazolium bromide (MTT) solution and counted colony number were per 6 microscopic fields. Each experiment was repeated two or three times.

2-2-10. RhoA activity assay

RhoA activity assay was performed and quantified using the RhoA activation assay kit based on rhotekin pull-down, according to the manufacturer's instructions (Cytoskeleton, Denver, Colorado, USA). Cells were stimulated with 100 ng/ml VEGF-A_{165} for 15 min. The cells were washed twice with cold PBS and lysed with Lysis buffer. The clarified cell lysate was incubated with Rhotekin-RBD protein agarose beads and rotated at 4°C for 90 min. The beads were washed once with wash buffer, samples were denatured and run on a SDS-gel. Active RhoA was detected by Western blot. The experiment was repeated three times and normalized by each total RhoA.

2-2-11. Immunohistochemistry (IHC)

The tumor sections were sliced 10 μm thick and the lymph nodes were sliced 8 μm thick using LEICA CM3050 S (LEICA, Wetzlar, Germany). Microvascular density (MVD) in the tumors was measured by CD31 staining. Tumor sections were fixed in 100% methanol at -20 °C for 20 min, washed with TBST and permeabilized in 0.3% Triton X-100 in TBS on ice for 10 min. The sections were blocked with 3% BSA/3% horse serum in TBST for 20 min, then incubated overnight with anti-mouse CD31 (1: 100) and anti-Keratin14 antibody (1: 500) diluted with blocking buffer. The sections were washed with TBST and incubated with Alexa-Fluor® 594 and 488-labeled secondary antibody (1: 100) for 1 h. After washing with TBST, the sections were mounted with DAPI containing mounting solution. Total CD31-positive areas were measured and analyzed by IPLab software. Photographs were taken with NIS-Elements (Nikon, Chiyoda-ku, Tokyo).

Ki67 staining was performed by Histofine® MOUSESTAIN KIT (Nichirei Biosciences Inc., Tokyo, Japan) followed as manufacture protocol. The tumor section was fixed with 4% paraformaldehyde for 20 min at room temperature and incubated with anti-Ki67 antibody (1: 100) and anti-Kertin14 antibody (1: 500) for overnight. The sections were incubated with anti-mouse 594 and anti-rabbit 488 antibodies (1: 100 respectively) for 1 h and mounted with DAPI-containing mounting solution. Confocal images of the tumor or lymph node were acquired by confocal microscope, Leica CTR5500 at x63 magnification.

2-2-12. Active-RhoA staining in tumor section

Staining of active-RhoA in the tumor section was based on *In situ* Rho[GTP] affinity assay performed by Berdeaux, R.L. et al[63]. Tumor section was washed with TBST containing 10mM $MgCl_2$ (TBST/$MgCl_2$) at three times and fixed with 100% methanol for 20min at -20°C. The section was blocked with 3% Horse serum /3% BSA in TBST/$MgCl_2$ for 30 min at 4°C. After blocking, the section was reacted with 50 μg/ml GST-tagged human recombinant Rhotekin-RBD protein (Cytoskeleton, Cat: #RT01) for 2 h at 4°C. Washed with TBST/$MgCl_2$, the section was incubated with anti-GST antibody (1: 100) and anti Keratin-14 antibody (1: 500) in blocking buffer for 1 h at room temperature (RT). Section was washed with TBST/$MgCl_2$ and incubated with biotin-conjugated anti-Hamster antibody (1: 200) for 45 min at RT. After incubation, section was washed with TBST/$MgCl_2$ and incubated with streptavidin-594 and anti-rabbit-488 antibody (1: 100, respectively) for 1h at RT. Nuclei was counterstaind with DAPI and mounted.

Confocal image of the tumor section was acquired by confocal microscope, LeicaCTR5500 at x63 magnification.

2-2-13. Transwell invasion assay

Invasion assays were performed for U87MG cells using Transwell inserts with 8.0 μm pore size (Corning, New York, USA), or for DJM-1 and PC3M cells using Millicell Cell Culture inserts with 12.0 μm (Millipore). Membranes were coated with 0.1 mg/ml Matrigel (Corning) for DJM-1 and U87MG cells or with 3.3 mg/ml for PC3M cells. Prior to the assay, the cancer cells were treated with siRNA (DJM-1 and PC3M cells: 20 nM, U87MG cells: 5 nM, respectively) for 20 hours or with peptide (500 nM) for 3 hours. One to 2×10^5 cells in appropriate culture media with 0.1% FBS were seeded into upper compartments and 0.1% FBS containing media were added into bottom chamber for suitable volume as description. After 24 to 48 hours, invaded cells were stained with Diff-Quick staining kit (SYSMEX, Kobe, Japan). The invaded cells to the lower side of the filter were counted under a phase contrast microscope. Averages were obtained from the 6 microscopic fields and the experiments were repeated 2 or 3 times. The means±s.d of invaded cells are shown.

2-2-14. Statistical analyses

All numerical data were expressed as the mean±standard error of the mean (SEM). A one-way analysis of variance (ANOVA) followed by with post-hoc analysis. Statistical analyses were analyzed with a two-tailed, paired Student's t-test, Bonferroni test and Tukey test in colony formation assay, ELISA, invasion assay, tumor volume and quantification of Immunohistochemistory. Incidence of lymph node metastasis was analyzed by Fisher's extract test. $^{\#}$, $^{\#\#}$, **, *** and N.S. stand for $P<0.05$, $P<0.01$, $P<0.005$, $P<0.001$ and "not significant", respectively.

2-3. Results

2-3-1. Inhibition of VEGF-A/NRP1-induced RhoA activation and cancer cell proliferation by cell-penetrating peptides corresponds to the Syx C-terminal region.

In chapter 1, I had shown that VEGF-A/NRP1 signaling activates RhoA to promote human skin cancer, prostate cancer, and glioblastoma proliferation under anchorage-independent conditions[56]. Figure 2-1A shows the cancer cells that expressed NRP1. I used human malignant skin cancer (DJM-1), glioblastoma (U87MG), and prostate cancer (PC3M) cell lines. All of cancers did not express VEGFR1 and VEGFR2. Figure 2-1A shows that DJM-1 (skin cancer), T98G (glioblastoma), U87MG (glioblastoma), HT1080 (fibrosarcoma) and PC3M (prostate cancer) expressed NRP1, but not expressed VEGFR1 and VEGFR2. I used DJM-1, U87MG, and PC3M for subsequent experiments. Additionally, U87MG expressed both NRP1 and NRP2 (**Fig. 2-1A**). PC3M cell was the highest expression of NRP1, whereas DJM-1 cell was the lowest. These cells secreted VEGF-A into the conditioned media (**Fig. 2-1B**). U87MG cells secreted the highest level of VEGF-A (45.6 ng/ ml/ 72 h).

These results suggested that the cancer cells expressed both NRP1 and VEGF-A, however did not express VEGFR1 and VEGFR2. There was no correlation with expression of NRP1 and VEGF-A secretion level in these cancer cells.

The addition of exogenous VEGF-A (100 ng/ml) activated RhoA activity in the siControl-treated cancer cells under anchorage-independent conditions (**Fig.2-1C**, siControl, +). On the other hand, treatment of siNRP1 suppressed VEGF-A-induced RhoA activation (**Fig. 2-1C**, siNRP1, +), suggesting that VEGF-A signals via NRP1 activate RhoA activity by autocrine manner in these cancer cells.

Molecular interaction of NRP1/GIPC1 and GIPC1/Syx were necessary to activate RhoA activity upon VEGF-A binding to NRP1 in the skin cancer cells[56]. To see if inhibition of RhoA activity suppresses cancer cell proliferation under anchorage-independent conditions, we generated the cell-penetrating peptides that consist of TAT, a cell penetrating sequence, EGFP, and eight amino acid residues including the Syx C-terminal region (STLTASEV: Targeted)[56]. Targeted peptide (Pep) interfered with the molecular interaction between the scaffold protein GIPC1 and RhoGEF; Syx. The Syx C-terminal region is important to recognize GIPC1 PDZ domain for GIPC1/Syx interaction[30], so the Targeted peptides (Pep) must act as competitive inhibitors to

block VEGF-A/NRP1 signaling to activate RhoA. The Scrambled peptide (Scr) was generated as a negative control for the Targeted peptide. By detecting EGFP fluorescence, internalization of the Scrambled or Targeted peptides into these cancer cells was confirmed after 24 hours of treatment (**Fig. 2-1D**). Peptide incorporation into cells was also confirmed for 1 to 48 h after treatment (data not shown). The Targeted peptides inhibited cell proliferation under anchorage-independent conditions in DJM-1 cells (45.5% of Scrambled), U87MG (59.3%) and PC3M (79.2%) respectively (**Fig. 2-1E**). The addition of exogenous VEGF-A did not stimulate RhoA activation in Targeted peptide-treated cancer cells, whereas VEGF-A did in Scrambled peptide-treated cancer cells (**Fig. 2-1F**). These results suggested that GIPC1/Syx interaction was necessary for anchorage-independent cell proliferation in these cancer cells.

2-3-2. The VEGF-A/NRP1 signaling promoted cancer cell invasion.

Up-regulation of RhoA activity may promote cancer cell invasion and metastasis, resulting in poor prognosis of cancer patients[64]. Whether the VEGF-A/NRP1 signal promotes cancer cell invasion, I evaluated by a Transwell invasion assay. These cancer cells expressed NRP1, GIPC1 and Syx, and those mRNA expressions were suppressed by siRNAs respectively **(Fig. 2-2A and Table 2-1)**. Conformation of siRNA efficiency in the cancer cells was performed by two different sequences (no.1 and no. 2) respectively. In **Figure 2-2A**, RT-PCR showed GIPC1 expression was high in U87MG and PC3M cells, besides high expression of Syx confirmed in DJM-1 and PC3M cells. siNRP1, siGIPC1 or siSyx treatment suppressed cancer cell invasion (**Fig. 2-2B**). The siRNA treatments inhibited cell invasion in DJM-1 cells (siNRP1 no. 1: 77% inhibition compared to siControl-DJM-1, no. 2: 75%, siGIPC1 no. 1: 69%, no. 2: 73%, siSyx no.1: 81%, no.2: 73% respectively), U87MG cells (siNRP1 no. 1: 50% inhibition compared to siControl-U87MG, no. 2: 71%, siGIPC1 no. 1: 93%, no. 2: 95%, siSyx no.1: 98%, no.2: 62% respectively), and PC3M cells (siNRP1 no. 1: 95% inhibition compared to siControl-PC3M, no. 2: 69%, siGIPC1 no. 1: 75%, no. 2: 85%, siSyx no.1: 91%, no.2: 93% respectively). These results indicated that the VEGF-A/NRP1 signaling-induced RhoA activation promoted cancer cell invasion.

Additionally, the Targeted peptide inhibited cancer cell invasion (**Fig. 2-2C,** DJM-1: 80.0% inhibition compared to Scrambled peptide treatment, U87MG: 52.2%, and PC3M: 53.3% respectively). Taken together, these results showed that the peptide that

inhibits the VEGF-A/NRP1 signal-induced RhoA activation was able to not only suppress cancer proliferation but also invasion.

2-3-3. NRP1 promoted cancer growth and lymph node metastasis.

Previously, we constructed a shNRP1 vector to abrogate the expression of NRP1 in DJM-1 cells[56]. One of stable shNRP1-DJM-1 clones (shNRP1-DJM-1 cell) that has no endogenous expression of NRP1, was orthotopically inoculated into nude mice. 5 weeks after the inoculation into the nude mice, the tumor volume of the shNRP-DJM-1 cells (shNRP1) was smaller than the shControl-DJM-1 cells (shControl) (**Fig. 2-3A**, 49.4% of shControl, P=0.039). Tumor-induced angiogenesis was evaluated by measuring the total $CD31^+$ area of the tumor sections at 2 weeks post inoculation. In shNRP1-DJM-1 tumors, tumor angiogenesis was strongly suppressed than in shControl-DJM-1 tumors (56% of shControl) (**Fig. 2-3B and C**). Regarding to metastasis, shControl-DJM-1 cells metastasized to the lymph nodes (4/13), whereas shNRP1 cells did not (0/14) (**Fig. 2-3D, P=0.041**). These results demonstrated that the NRP1 promoted tumor growth and metastasis *in vivo*, however, tumor angiogenesis in the tumors of shNRP1-DJM-1 cells was suppressed, so it should be elucidated whether this phenomenon is due to the lack of NRP1 signal in the cancer cells and/or to the low induction of tumor-angiogenesis as shown in Fig.2-3B and C.

2-3-4. NRP1 cytoplasmic region was essential for cancer cell proliferation and invasion.

To elucidate the role of the VEGF-A/NRP1 signaling in cancer cell proliferation and invasion, shNRP1-DJM-1 cell clones were infected with NRP1WT or NRP1 mutant that lacks the C-terminus amino acids, SEA (NRP1ΔSEA) **(Fig. 2-4A and B)**. In soft agar assay, the cell proliferation of the shNRP1 clone was lower than that of the shControl clone (56% of shControl) **(Fig. 2-4C)**. The lentiviral overexpression of NRP1WT in the shNRP1 clone restored growth, whereas that of NRP1ΔSEA did not (shNRP1+WT: 129% of shControl, shNRP1+ΔSEA: 60%, respectively) **(Fig. 2-4C)**. Additionally, RhoA activity was restored in NRP1WT (130% of shControl) compared to shNRP1 (55%), whereas that in shNRP1ΔSEA was not recovered (54%) **(Fig. 2-4D)**. Furthermore, NRP1 signal promoted cancer cell invasion **(Fig 2-4E)**. As well as siNRP1 treatment in **Fig. 2-2B**, the invasion of shNRP1-DJM-1 cells was inhibited compared to that of shControl cells (16%). Whereas

lentiviral overexpression of NRP1WT promoted invasion (77%). shNRP1ΔSEA overexpression slightly restored cancer cell invasiveness, but there is no significant difference compared to shNRP1 (33% of shControl). These results suggested that the NRP1 cytoplasmic region, containing SEA, was essential for VEGF-A-induced proliferation and invasiveness.

2-3-5 The NRP1 cytoplasmic region was important for tumor growth and lymph node metastasis *in vivo*.

Figure. 2-4 showed the importance of NRP1 cytoplasmic region to cancer cell proliferation and invasiveness *in vitro* assays, so the effects of NRP1 cytoplasmic region in tumor growth and metastasis were examined *in vivo*. The shControl-, shNRP1-, shNRP1WT- or shNRP1ΔSEA-DJM-1 cells were olthotopically inoculated into nude mice. 17 days after the inoculation, the tumor volume of the shNRP-DJM-1 cells (shNRP1) was smaller than that of the shControl-DJM-1 cells (shControl) (69% of shControl, P=0.60) (**Fig. 2-5A**). Moreover, overexpression of NRP1WT in the shNRP1-DJM-1 cells (shNRP1+WT) restored tumor volume compared to shControl and shNRP1 (140%, P=0.115 compared to shControl, 203%, P=0.036 compared to shNRP1, respectively), whereas NRP1ΔSEA-DJM-1 cells (shNRP1+ΔSEA) slightly recovered tumor volume (80% of shControl, P=0.793) (**Fig. 2-5A**). Tumor-induced angiogenesis was evaluated by measuring the total $CD31^+$ area of the tumor sections at 2 weeks post inoculation (**Fig. 2-5B and C**). In shNRP1-DJM-1 tumors, tumor angiogenesis was more suppressed than in shControl-DJM-1 tumors (46% of shControl), whereas there were no significant difference in angiogenesis between the shControl-DJM-1, shNRP1 +WT and +ΔSEA-DJM-1 tumors (+WT: 95%, +ΔSEA: 96% of shControl, respectively) (**Fig. 2-5B and C**). These results demonstrated that the overexpression of NRP1WT or NRP1ΔSEA increased tumor angiogenesis equally. shControl-DJM-1 cells metastasized to the lymph nodes (7/24, incidence: 29%); however, the metastasis of shNRP1-DJM-1 cells was completely inhibited (0/24, P=0.009 vs shControl, **Fig. 2-5D and Table 2**). Furthermore, overexpression of NRP1 WT in shNRP1 cells, lymph node metastasis was significantly restored to 0% to 32% compared to shNRP1 (6/19, incidence: 32%, P=0.005 vs shNRP1, **Fig. 2-5D and Table 2**). On the other hand, the metastasis of NRP1ΔSEA-expressed shNRP1 cell to lymph node was suppressed than that NRP1WT-expressed shNRP1 cells (1/21, incidence: 5%, P=0.478 vs shNRP1, **Fig. 2-5D**

and Table).

To asess whether RhoA was activated in NRP1 expressed cancer cells in vivo, tumor sections obtained from those tumors after 2 weeks inoculation and stained for active form-RhoA using with GST-fused rhotekin protein. Due to active form-RhoA could bind rhotekin, which is a downstream molecule of RhoA, RhoA activity in tumor section was detected by immunostaing for GST-fused rhotekin protein[63]. The active RhoA (red) was increased in shControl-DJM-1 (shControl) tumor section, but it was decreased in shNRP1 tumor (31% compared to shControl) **(Fig. 2-5Ea, b)**. Whereas shNRP1 +WT tumor restored active RhoA compared to shNPR1 tumor, and shNRP1+ΔSEA tumor did not restore RhoA (WT: 104%, ΔSEA: 43% compared to shCointrol respectively) **(Fig. 2-5Ec, d)**. Corresponding to the RhoA activation, positive cell stained with Ki67, a proliferation marker (red), were increased in shControl and shNRP1 +WT (shNRP1: 60%, WT: 96%, ΔSEA: 53% compared to shControl respectively) **(Fig. 2-5Ee-h)**. These results suggested that the cytoplasmic region of NRP1 plays a crucial role for transducing VEGF-A-induced proliferative, invasive signals that activated RhoA activity and promoted tumor growth and metastasis *in vivo*.

2-4. Figure and Legends.

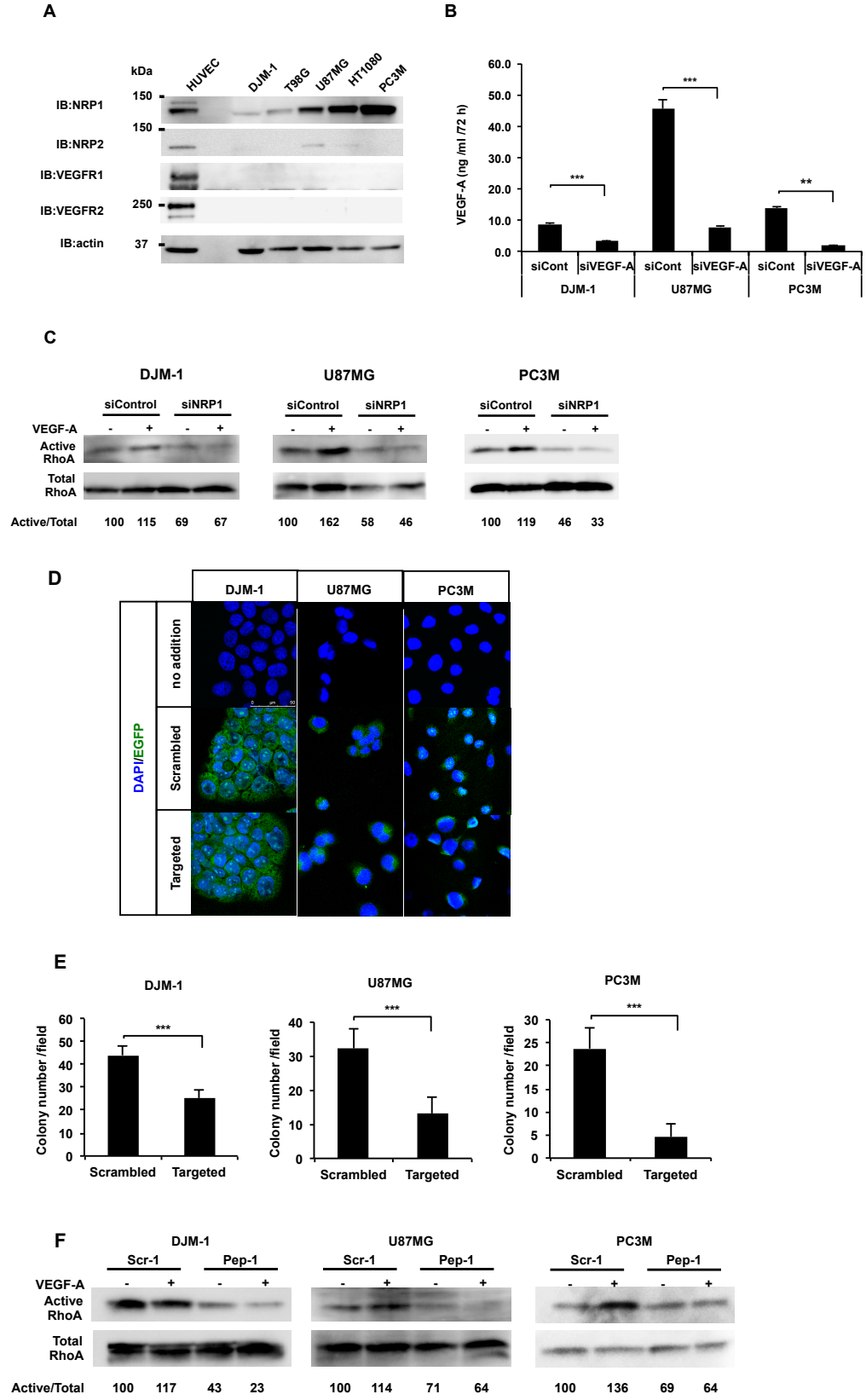

Figure 2-1. Cell-penetrating peptides which abrogate GIPC1 interaction with Syx and inhibited cancer cell proliferation and RhoA activation in anchorage-independent condition.

(A) Western blot showing NRP1, NRP2, VEGFR1 and VEGFR2 expression in DJM-1 (human skin cancer), T98G, U87MG (both Glioblastoma), HT1080 (fibrosarcoma), and PC3M (prostate cancer) cells. The cell lysates were quantified for protein concentration and subsequently loaded on a 6 % SDS-polyacrylamide gel. (B) VEGF-A ELISA. After VEGF-A siRNA treatment (5 nM) for overnight, cancer cells were cultured with 1% BSA-containing each basal medium for 72 h. Conditioned media were diluted to 10-fold by serum free medium and analyzed VEGF-A concentration. Each sample was duplicated. The experiment was repeated twice and the data represent the means ± S.D. (C) RhoA activity assay. Cancer cells were treated with siControl or siNRP1 and growing in the presence (100 ng/ml) (+) or absence of exogenous VEGF-A (-) on polyHEMA-coated plates. Subsequently the cell lysates were collected and analyzed for RhoA activity. (D) Confirmation of peptides incorporation into the cancer cells. After 24 h treatment with the target peptide or scrambled peptide (500 nM), cells were fixed with 100% methanol and peptide incorporation was detected by green fluorescent protein. Scale bar; 50 μm. (E) Peptide inhibited cancer cell proliferation in anchorage-independent condition. The cancer cells were plated in soft agar and treated with Targeted peptide or Scrambled peptide. The cells were incubated for 2 weeks and stained with MTT solution. Viable colonies (DJM-1: larger than 80 μm diameter, U87MG and PC3M: larger than 30 μm diameter) per microscopic field were counted. Six fields were counted and these data represent the means ± S.D. (F) RhoA activity assay. The Targeted peptide inhibited RhoA activation of the cancer cells in anchorage-independent condition. Cancer cells were seeded on polyHEMA-coated dishes and treated with Scrambled or Targeted peptide for 24 h. The cells were stimulated in the presence (100 ng/ml) (+) or absence of exogenous VEGF-A (-). The cell lysates were collected for RhoA activity assay. Percentages from each mean relative to the siControl (-) or Scrambled peptide (-) are shown below the graph. **P<0.005, ***P<0.001.

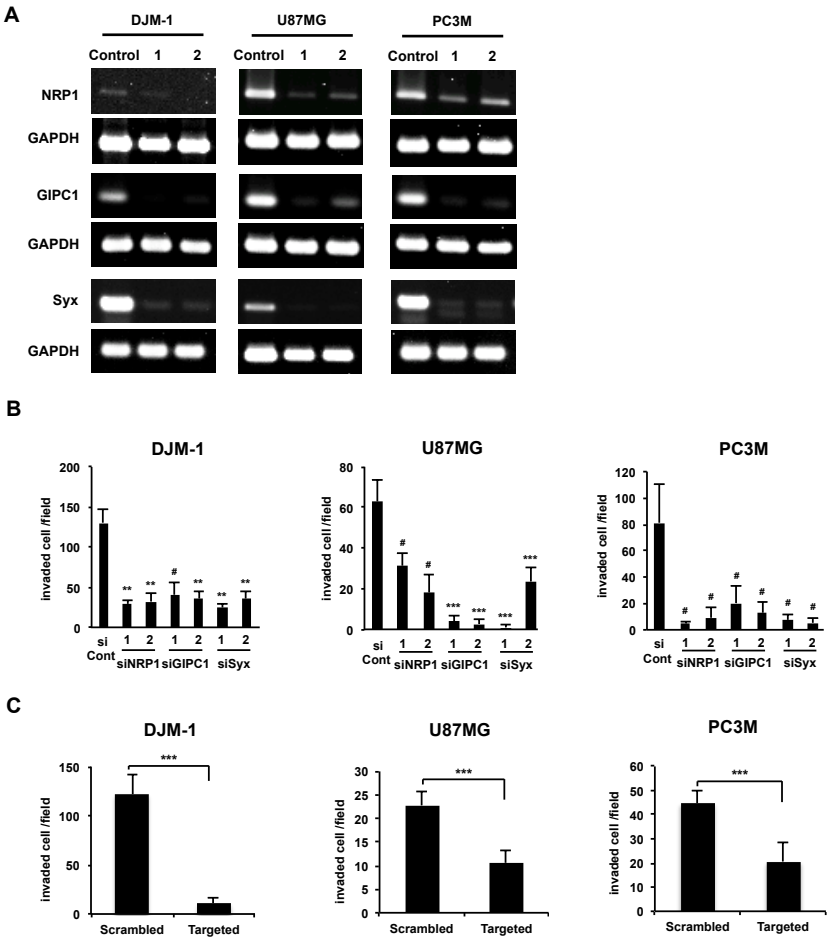

Figure 2-2. NRP1 and downstream molecules, GIPC1 and Syx promoted malignant cancer cells invasion.

(A) RT-PCR analysis for expression of NRP1, GIPC1 or Syx in cancer cells. The cancer cells were treated with 20nM siRNA for 72 h and isolated RNA. 1 and 2 are indicates treatment for distinct siRNA sequence respectively. GAPDH as a loading control. (B) Transwell invasion assay. Cancer cells were treated with 20 nM siRNAs for overnight and were seeded into upper cup. After 16 or 48 h, invaded cells were counted. Mean number of cells that invaded in a matrigel-coated Transwell membrane was shown. Six fields were counted for each condition and these data represent the means ± S.D. (C) Transwell invasion assay. The cancer cells were treated with 500 nM of Targeted or Scrambled-peptides and cultured for over night before tested. Mean number of cells that invaded in a matrigel-coated Transwell membrane was shown. Six fields were counted for each condition and these data represent the means ± S.D. $^{\#}$P<0.05; **P<0.005, ***P<0.001.

siRNA	sequence (5’-3’)
siGIPC1 no.1	Sense: 5’-GGCCGUACCUUCACGCUGATT-3'
	Antisense: 5’-UCAGCGUGAAGGUACGGCCTT-3'
siGIPC1 no.2	Sense: 5'-GCAAGGCCUUCGACAUGAUTT-3'
	Antisense: 5'-AUCAUGUCGAAGGCCUUGCTT-3'
siSyx no.1	Sense: 5'-UCAAGUCGGUGCUGAGGAATT-3'
	Antisense: 5'-UUCCUCAGCACCGACUUGATT-3'
siSyx no.2	Sense: 5'-GACCAAGAGACAGCAGACATT-3'
	Antisense: 5'-UGUCUGCUGUCUCUUGGUCTT-3'

Table 2-1. Targeting sequences of siRNA.

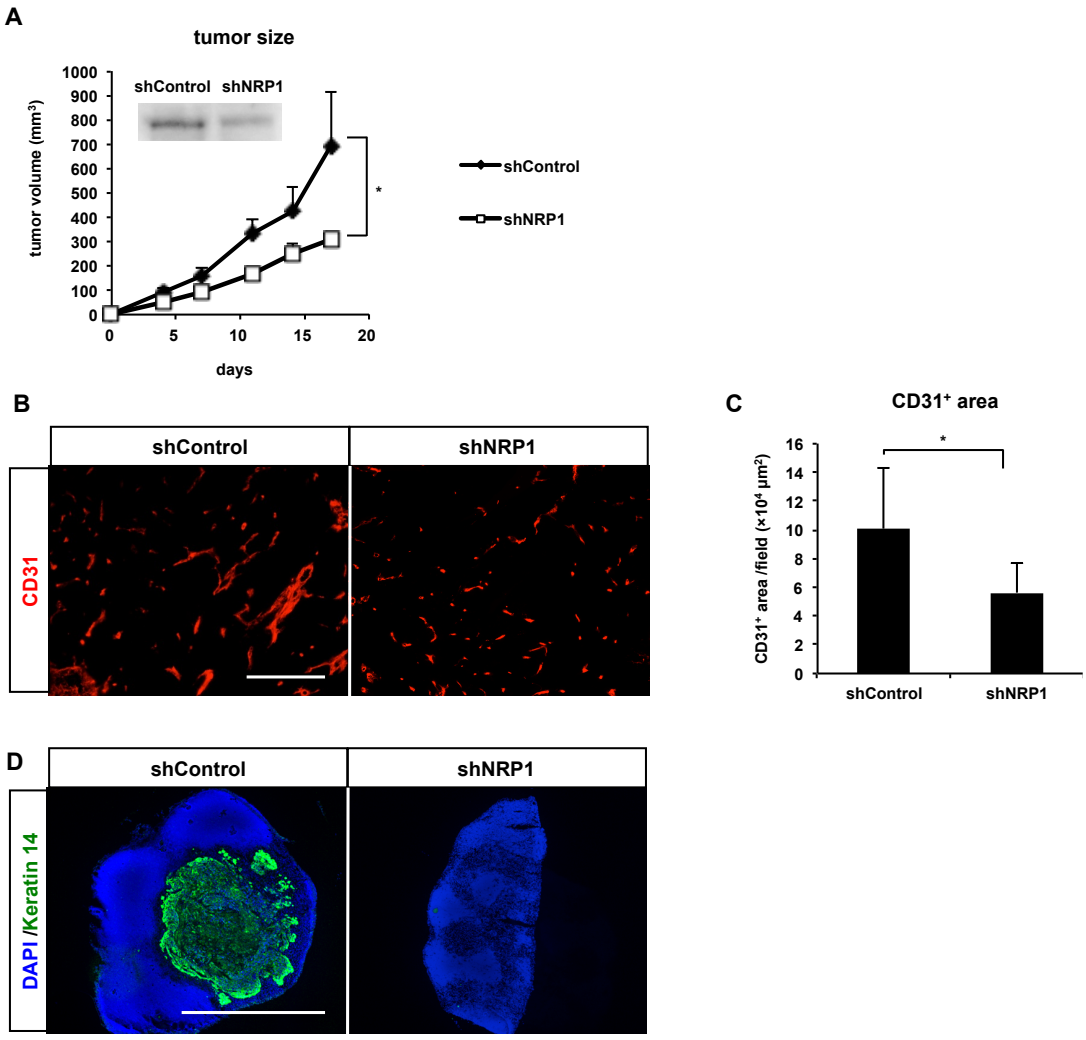

Figure 2-3. NRP1 promoted cancer growth and lymph node metastasis.

(A) Tumor growth in vivo. $4x10^6$ of shControl-treated or shNRP1-treated DJM-1 cells were olthotopically inoculated at the right flank of the mice and the means of tumor volumes were shown at the time indicated after injection (n=4). These data represent the means ± S.D. (B) Tumor sections isolated to 2 weeks after inoculation were stained with anti-CD31 antibody (endothelial cell marker: Red). Scale bar: 100 μm. (C) Graph showed total $CD31^+$ area of (B) in these tumor sections measured by IP Lab. The data represent the means ± S.D. (D) Proximal lymph nodes isolated to 5 weeks after inoculation were stained with anti-Keratin 14 antibody (epithelial marker: Green, DAPI: Blue, P=0.041). Scale bar: 100 μm. Four mice were analyzed and these data represent the means ± S.D. *P<0.05.

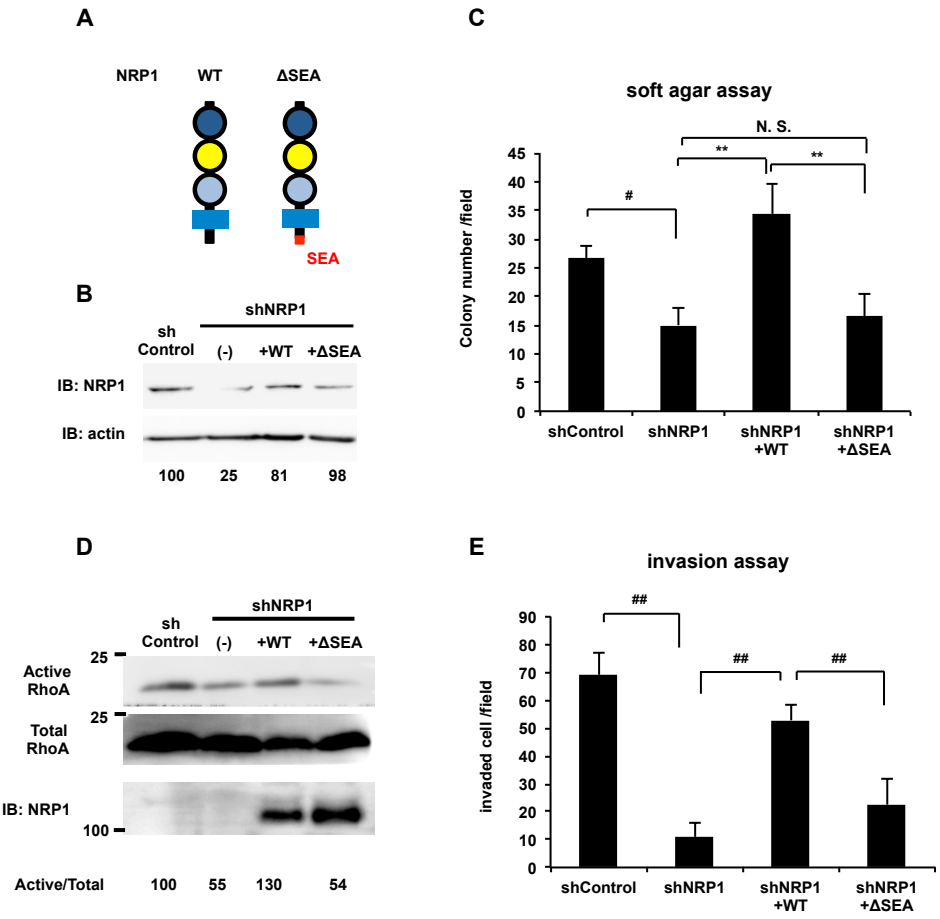

Figure 2-4. NRP1 cytoplasmic region was essential for cancer cell proliferation and invasion.

(A) Schematic of NRP1 wild type and ΔSEA structure. ΔSEA lacks three amino acids of NRP1 C terminus, Ser-Glu-Ala. (B) Western blot for NRP1WT or NRP1ΔSEA expression in shNRP1-DJM-1 cells. Infection of NRP1WT or NRP1ΔSEA virus in shNRP1-DJM-1 cells and these cells were used for soft agar assay in (C). (C) Soft agar assay of NRP1WT or NRP1ΔSEA-shNRP1 DJM-1 cells. Colonies were counted 6 fields and these data represent the means ± S.D. (D) RhoA activity assay. shNRP1-DJM-1 cell infected with NRP1WT or NRP1ΔSEA were seeded on poly-HEMA-coated dish. Incubated for overnight, the cells were analyzed RhoA activity. (E) Transwell invasion assay. Overexpressed NRP1WT or NRP1ΔSEA in shNRP1-DJM-1 cell and were seeded into matigel-coated transwell. Six fields were counted and the data representative means ± S.D. Percentages from each mean relative to the shControl are shown below the graph. N.S., not significant, $^{\#}P<0.05$; $^{\#\#}P<0.01$; **P<0.005, ***P<0.001.

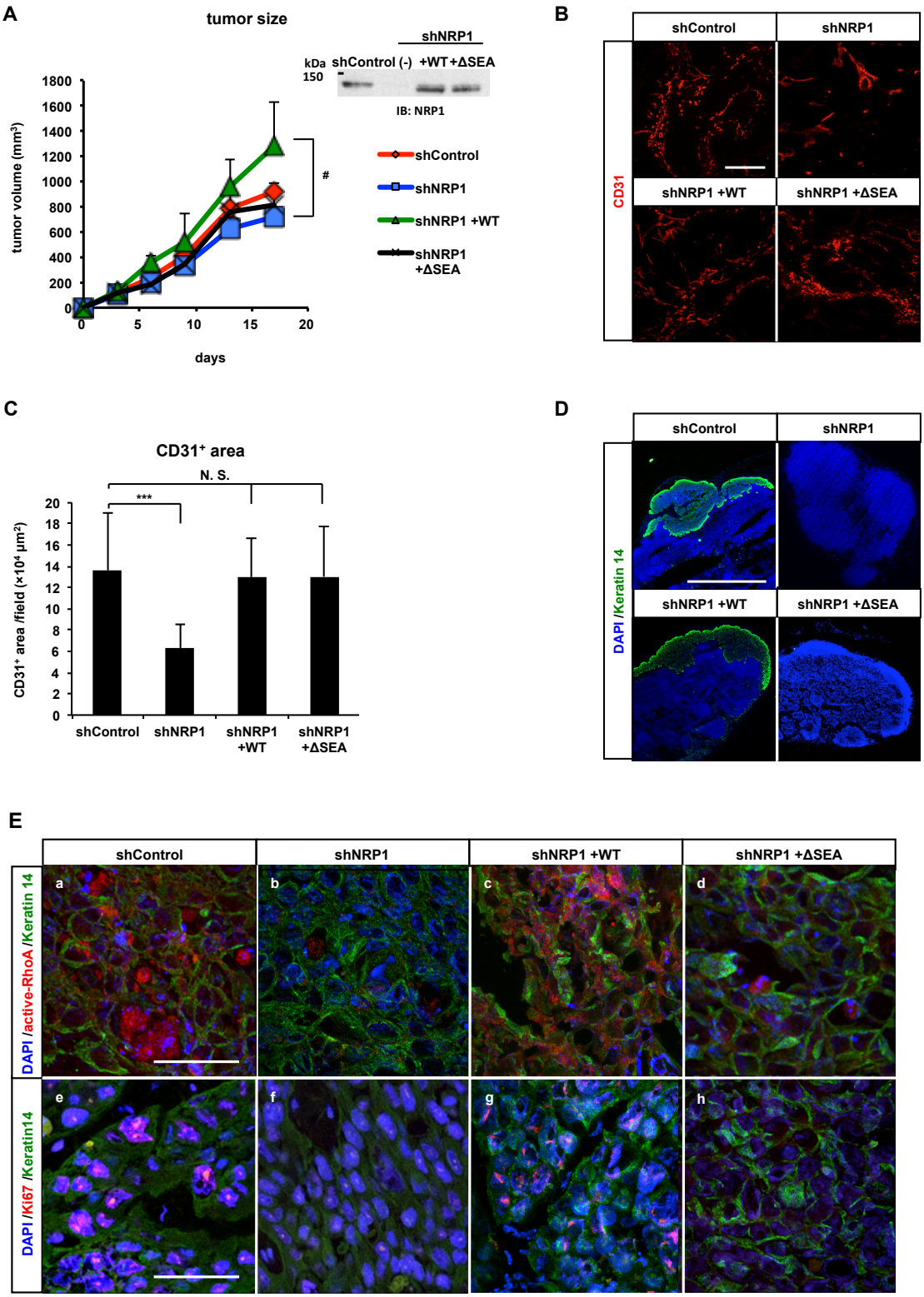
A
tumor size
shNRP1
kDa
150
shControl (-)
+WT
+ΔSEA
IB: NRP1
tumor volume (mm³)
1800
1600
1400
1200
1000
800
600
400
200
0
0
5
10
15
20
days
#
shControl
shNRP1
shNRP1 +WT
shNRP1 +ΔSEA
B
shControl
shNRP1
CD31
shNRP1 +WT
shNRP1 +ΔSEA
C
CD31⁺ area
N. S.
***
CD31⁺ area /field (×10⁴ μm²)
20
18
16
14
12
10
8
6
4
2
0
shControl
shNRP1
shNRP1 +WT
shNRP1 +ΔSEA
D
shControl
shNRP1
DAPI /Keratin 14
shNRP1 +WT
shNRP1 +ΔSEA
E
shControl
shNRP1
shNRP1 +WT
shNRP1 +ΔSEA
DAPI /active-RhoA /Keratin 14
a
b
c
d
DAPI /Ki67 /Keratin14
e
f
g
h

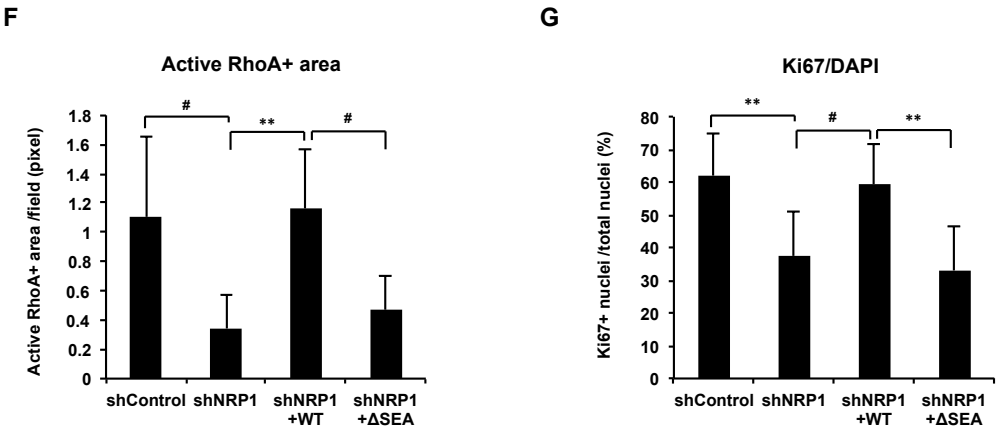

Figure 2-5. NRP1 cytoplasmic region was important to cancer cells for lymph node metastasis *in vivo*.

(A) Tumor growth *in vivo*. 4×10^6 cells of shControl-treated DJM-1 clone, shNRP1-treated DJM-1 clone or shNRP1-treated and NRP1 WT or NRP1ΔSEA infected DJM-1 clone (shNRP1ΔSEA) were olthotopically inoculated at the right frank of the mice. The means of tumor volumes were shown at the time indicated after injection. (n=6). (B) Tumor sections isolated to 2 weeks after inoculation were stained with anti-CD31 antibody (endothelial cell marker: Red). Scale bar: 100 μm. (C) Graph showed total $CD31^+$ area of (B) in these tumor sections measured by IP Lab. The data represent the means ± S.D. (D) Proximal lymph nodes isolated to 5 weeks after inoculation were stained with anti-Keratin 14 antibody (epithelial marker: Green, DAPI: Blue). Scale bar: 100 μm. (E) (a-d) Active-RhoA staining in DJM-1 tumor section. The section were incubated with GST-fused Rhotekin protein and stained with anti-GST antibody (red) and anti-Keratin 14 antibody (Green). Scale bar: μm. (F) is shown quantitative analysis of (Ea-d). (e-h) Ki67 staining in DJM-1 tumor section. The section were stained with anti-Ki67 antibody (red) and anti-Keratin14 antibody (Green). Scale bar: 50 μm. (G) is shown quantitative analysis of (Ee-h). N.S., not significant, $^{\#}P<0.05$; *P<0.05, ***P<0.001.

	Incidence of lymph metastasis	%	P-value
shControl	7/24	29	
shNRP1	0/24	0	0.0094*
shNRP1 +WT	6/19	32	0.0045**
shNRP1 +ΔSEA	1/21	5	0.4783**

Table 2-2. NRP1 cytoplasmic region was important to cancer lymph node metastasis.

Incidence of lymph node metastasis from Figure 2-5D. *, compared to shControl: **, compared to shNRP1.

2-5. Discussion

The data presented here that cancer cell-secreted VEGF-A activated RhoA via NRP1 to up-regulate the tumorigenic activity in an autocrine manner and supported the existence of the commonality of the VEGF-A/NRP1 signaling pathway in many types of cancer cells. Beck, B. et al. demonstrated that VEGF-A/NRP1 stimulated the stemness of squamous skin tumors and promoted skin cancer initiation[13]. Cao, Y. et al showed that suppression of VEGF-A expression by shRNA decreased tumor volume and inhibited cancer cell survival through Ras inactivation in two human renal cell carcinoma cell lines[9].

Diminished endogenous expressions of NRP1, GIPC1 and Syx by siRNAs in human cancer-derived cell lines, DJM-1, skin cancer, U87MG, glioblastoma and PC3M, prostate cancer suppressed VEGF-A-induced RhoA activation, anchorage-independent proliferation and cancer cell invasiveness. These cancer cell lines did not express VEGFR1, VEGFR2 and VEGFR3. The expression level of NRP1 has no correlation with cancer proliferation, invasion and RhoA activity. For instance, DJM-1 cell was the lowest expression of NRP1 in cancer cells, however, the abilities of colony formation and invasion in DJM-1 cells is stronger than those in PC3M cells that expressed the highest level of NRP1. Thus, the upregulation of the downstream molecules of VEGF-A/NRP1 signal such as GIPC1 and Syx may promote cell proliferation and invasiveness through RhoA activation. Up-regulation of GIPC in breast, ovarian, gastric, and pancreatic cancers[25] has been reported. In breast cancer, GIPC1 promoted cancer invasion by interacts with MyoGEF [26]. Syx was also expressed in glioblastoma, skin, breast and prostate cancer [30, 55]. Syx promoted breast cancer migration [55].

In Chapter 2, it was shown that VEGF-A-induced GIPC1/Syx complex formation may lead to activate RhoA and promote cancer cell proliferation and invasiveness. Cell-penetrating peptides corresponding to the sequences of eight amino acids of Syx C-terminus (STLTASEV) interfering with GIPC1 interaction inhibited cell proliferation and invasion in the cancer cells. The target sequences of the peptide, especially the C-terminal 3 amino acids SEV, are essential[18,30]. In fact, MyoGEF, another activator of RhoGTPase, has SEV as the C-terminal 3 amino acids sequence, which interacts with GIPC1 to promote breast cancer cell invasion[26]. To elucidate which is more effective to inhibit the VEGF-A/NRP1 signal, two peptides corresponding to NRP1 C-terminus

sequences, containing SEA (targeting NRP1/GIPC1 interaction), or Syx C-terminal sequences, SEV (targeting GIPC1/Syx interaction) were generated. As a result, targeting GIPC/Syx interaction inhibits cancer cell proliferation and invasion more effective than that of NRP1 /GIPC1 one (data not shown). It might be possible that inhibition of RhoA, a key event as the downstream signal of VEGF-A/NRP1 directly regulated by Syx RhoGEF is more effective to suppress the cancer cell activities compared to the interference of NRP1/GIPC1. To date, there have been many reports indicating that many types of cancer cells express NRP1 and GIPC1[6,11,25,27,51,65-68]. The motif in the C-terminus of NRP1 and RhoGEFs may be important to transduce the signaling of VEGF-A secreted by cancer cells. Contributions of RhoGEFs, including Syx, to cancer progression have been implicated in the activation of small GTPases, such as RhoA. Numerous reports indicates the involvement of RhoGEFs and cancer progression: Ect2 in lung cancer and esophageal cancer, Net1 in gastric cancer, Vav in neuroblastoma and melanoma[69-72]. RhoA is a well-known regulator of the actin cytoskeleton and enhances the cell motility responsible for cancer cell invasion and metastasis[64,73]. Thus, VEGF-A/NRP1 signaling in cancer cells followed by RhoA activation via the molecules GIPC1 and Syx, RhoGEF, may be conserved among different types of cancer.

Tumor angiogenesis is important for tumor growth and metastasis[74,75]. NRP1 acts as VEGF-A reservoir and thus, promotes tumor angiogenesis[52]. The extracellular domain of NRP1 expressed in cancer cells has been reported to aid the enrichment of VEGF-A in the peri-tumor environment to induce tumor angiogenesis[8]. On the other hand, Gerreti. et al demonstrated soluble NRP consisting with NRP extracellular domain inhibited tumor growth, but not affect microvascular density in tumor[76]. In this study, the diminished expression of NRP1 in shNRP1-DJM-1 cells resulted in less tumor volume with poor blood vessel formation as compared to shControl-DJM1 cells *in vivo*. Overexpression of NRP1WT in shNRP1-DJM-1 cells was increased tumor volume and restored tumor angiogenesis, however NRP1ΔSEA, lacking the intracellular domain of NRP1, did recover tumor angiogenesis to the level of shControl-DJM-1 tumor, although the tumor volume of shNRP1 +ΔSEA-DJM-1 tumors did not recover to the level of the shNRP1 +WT-DJM-1 tumor volume. However, the tumors of the shNRP1+ΔSEA-DJM-1 cells suppressed metastasis to proximal lymph nodes, while the shControl and shNRP1 +WT DJM-1 cells did. In general, Tumor angiogenesis promotes tumor growth and

metastasis; however, NRP1 might promote tumor metastasis by tumor angiogenesis independently. Snuderl et al. showed overexpression of NRP1ΔSEA was suppressed medulloblastoma proliferation and infiltration[11]. In invasiveness, NRP1 regulates MMP secretion in cancer cells[67,77]. Additionally, RhoA promotes cell motility and stimulates MMP secretion in tongue cancer[78]. So, the VEGF-A/NRP1 signal activates RhoA, NRP1 expressed-cancer cells might be promoted proliferation, but also invasiveness and metastasis by tumor angiogenesis-independent manner.

These results suggest that VEGF-A has two functions via the extracellular and intracellular regions of NRP1: (1) to supply blood vessels to tumors; (2) to signal proliferative and invasive activities to cancer cells.

In conclusion, VEGF-A-induced GIPC1 interaction with Syx, and NRP1 plays a key role for RhoA activation, to enhance cancer progressive activities such as proliferation, invasion and metastasis. Strategies to inhibit the signaling pathway are promising for the creation of new cancer therapeutic drugs.

General discussion

This study demonstrated that Neuropilin-1 (NRP1) promoted cancer cell proliferation, motility, invasion and metastasis by autocrine VEGF-A stimulation. The VEGF-A/NRP1 signal-induced complex formation between GIPC1 and Syx and activated a member of small G protein, RhoA, which is a regulator of cell proliferation, migration, and invasion. Activation of RhoA promoted degradation of p27, a cyclin-dependent kinase (CDK) inhibitor, resulting in acceleration of cancer cell proliferation and rearrangement of actin cytoskeleton, leading to up-regulation of cancer cell invasion (**Figure 3**).

In this study, skin, brain, and prostate cancer cells expressed VEGF-A and NRP-1, creating autocrine loop to stimulate cell proliferation and invasion. Other groups also reported that NRP1 promoted cell proliferation, migration, and invasion in lung cancer [79], ovarian cancer [80], glioblastoma [81-83], medulloblastoma [11].

Not only NRP1 but also NRP2 has shown to have an important role in cancer progression. Lee Ellis and his research group has shown that NRP2 has an important role in progression of colorectal cancer[84]. Also, NRP2 has shown to be overexpressed in breast cancer[85].

NRP2 expression was also observed in prostate, breast, pancreatic, and melanoma, renal cell carcinoma, osteosarcoma, glioblastoma and lung cancers. In prostate cancer, NRP2 accelerated tumor growth and metastasis[86]. NRP2 promoted breast cancer initiation, and proliferation and metastasis[85,87]. In melanoma, NRP2 promoted tumor growth and tumor-angiogenesis[76]. NRP1 and NRP2 promoted lung cancer tumor-angiogenesis and progressed NSCLC, results in poor prognosis[88 89].

In this study, although U87MG glioblastoma cells expressed NRP2, siRNA knockdown of NRP1 inhibited 94% of cell invasion, suggesting the VEGF-A through NRP1 signaling predominantly stimulate cell invasiveness in U87MG. In addition, siVEGF-A or siNRP1 inhibited cell proliferation at the similar levels in U87MG cells, indicating that NRP1 mainly mediates VEGF-A signal to promote cell proliferation in the cells.

As shown in this study, NRP1 cytoplasmic region was crucial for the VEGF-A-induced RhoA activation, cancer cell proliferative and invasive signals. NRP1 cytoplasmic region consists of 44 amino acids including the C-terminus three amino acids, Ser-Glu-Ala (SEA), which needs to bind GIPC1 that has a function as a scaffolding protein[90]. The

interaction between NRP1 cytoplasmic region and GIPC1 is necessary to transduce VEGF-A signaling in cancer cells. Syx is a RhoA specific GEF and has been reported to bind to GIPC1. In the present study, it was shown that VEGF-A binding to NRP1 triggers complex formation between GIPC1 and Syx to activate RhoA.

Bachelder has shown that VEGF-A acts as an autocrine survival factor for breast carcinoma cells through a NRP1-dependent activation of the Akt survival pathway[17]. Overexpression of NRP1 in renal cell carcinoma and breast cancer cells enhanced Ras/MAPK signaling[9]. In pancreatic cancer cells, NRP1 promoted MAPK signaling and chemoresistance[91]. However, in the present study, knockdown of VEGF-A or NRP1 did inhibit RhoA activation, but not MAPK and Akt pathways in skin cancer cells.

In many types of cancer patients, NRPs were correlated with tumor aggressiveness, advanced disease stage and poor prognosis: Lung cancer[79], ovarian cancer[80], colon cancer, gastrointestinal cancer[92,93], glioblastoma, medulloblastoma[11,81-83], prostate cancer[94 95], breast cancer[96], [97], Pancreatic cancer[98 99], [91].

Therefore, it is intriguing to develop the inhibitor of VEGF-A/NRP1 signaling for molecular target cancer drug therapies.

First, as a strategy in cancer therapy, targeting of NRP1 extracellular domain has been demonstrated. Anti-NRP1 antibody that inhibits VEGF-A/NRP1 interaction was generated by Genentech suppressed tumor angiogenesis and tumor growth in advanced solid tumors. Anti-NRP1 antibody prevented blood vessel maturation; thereby keep vessels inside of tumor and more sensitive for anti-VEGF therapy. Phase I study showed anti-NRP1 antibody was well tolerated in cohorts and enhanced anti-tumor effect by bevacizumab, blockage of VEGF [100,101].

Soluble-NRP that was genetically modified NRP2 B domain to increase an affinity with VEGF-A than wild-type NRP1 B domain inhibited VEGF-A/NRP1 binding and suppressed tumor-angiogenesis and tumor growth in melanoma xenograft model[76]. EG3287, a bicyclic peptide based on a NRP1 binding site located in VEGF exons 7 and 8, selectively inhibited VEGF-A binding to NRP1 and inhibited phosphorylation of VEGFR2 in endothelial cell. EG3287 inhibited adhesion lung carcinoma, kidney carcinoma and prostate cancer cell to extracellular matrix and immigration and increased sensibility for 5'-FU and cisplatine, chemotherapeutic agents[102]. Tuftsin, an analogue of VEGF exon 8 consisting 4 amino acids, inhibited VEGF-A binding to NRP1 and inhibited VEGF-A/NRP1/VEGFR2 signaling in endothelial cell and aortic cells [103]. Another peptide,

ATWLLPR (A7R), inhibited VEGF-A binding to NRP1 but not to VEGFR-2 and inhibited endothelial cell proliferation and vessel formation and suppressed breast cancer growth[104].

Second, targeting for NRP1 cytoplasmic region might be useful for anti-cancer strategies. Recently, Patra CR, et al. has reported a chemically modified-cell penetrating octapeptide targeting to the PDZ domain of GIPC and inhibited interaction with IGF-IR and GIPC1. The peptide down-regulated EGFR and IGF-IR expression, consequently induced apoptosis, suppressed proliferation and tumor growth in breast and pancreatic cancer cells[105].

This study showed a new approach to inhibit cancer progression. Cell-penetrating peptides corresponding to the sequences of eight amino acids of Syx C-terminus competitively interfere with GIPC interaction with Syx inhibited RhoA activation, cell proliferation and invasion of cancer cells. To inhibit RhoA activation, a key event as the downstream signal of VEGF-A/NRP1 directly, the interference of GIPC and Syx RhoGEF interaction is more effective to suppress the cancer cell activities compared to that of NRP1 and GIPC1 interaction. Further modifications of the cell-penetrating peptides for higher affinity to the target molecules and longer half-life may contribute to increased effectiveness on inhibition of tumorigenic activities.

These findings provide strong evidence for the importance of VEGF-A-binding to NRP1 in cancer cell proliferation, invasion, and metastases in vivo. Targeting to the VEGF-A/NRP1 signaling molecules will be powerful means for developing new cancer therapeutic drugs.

Figure 3.

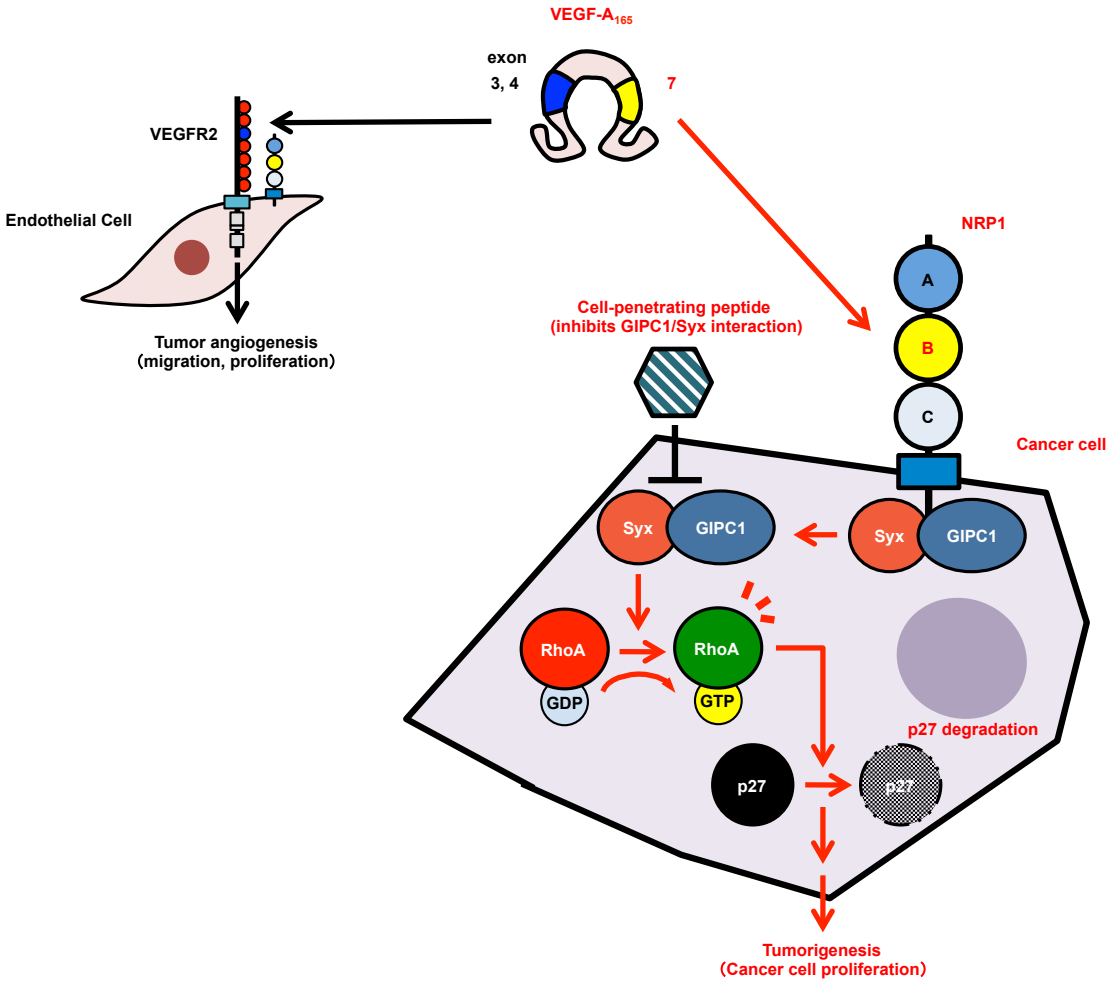
VEGF-A165
exon
3, 4
7
VEGFR2
Endothelial Cell
Tumor angiogenesis
(migration, proliferation)
NRP1
A
B
C
Cell-penetrating peptide
(inhibits GIPC1/Syx interaction)
Cancer cell
Syx
GIPC1
Syx
GIPC1
RhoA
GDP
RhoA
GTP
p27 degradation
p27
p27
Tumorigenesis
(Cancer cell proliferation)

Acknowledgments

The present thesis is a summary of my studies from 2012 to 2015 at the Department of Biotechnology, Faculty of Engineering, Kyoto Sangyo University.

I would like to express my sincere gratitude to my supervisor, Professor Misuzu Seo of the Laboratory of Vascular and Neuronal Biology, Department of Molecular Biosciences, Faculty of Life Sciences, Kyoto Sangyo University, for providing me this precious study opportunity as a Ph.D student in her laboratory. This study could not achieve without her guidance, incisive suggestions, invaluable discussion and sincere encouragement.

I especially would like to express my deepest appreciation to Dr. Akio Shimizu for his elaborated guidance, and stimulating discussion considerable encouragement that make my research of great achievement and my study life unforgettable.

I would like to gratefully thank Professor Michael Klagsbrun of the Vascular Biology Program, Boston Children's Hospital, Departments of Surgery and Pathology, Harvard Medical School for scientific advice and Ms. Melissa Anderson for support preparation of my doctoral thesis.

I wish to thank Professor Shinae Kondoh and Associate Professor Tetsuya Kadonosono for their valuable cooperation in my experiments. Dr. Elena Geretti and Dr. Akiko Mammoto of Vascular Biology Program, Departments of Pathology & Surgery, Boston Children’s Hospital and Harvard Medical School kindly providing me soluble NRP DNA construct and constitutively active RhoA DNA construct respectively.

I appreciate Nobuhiro Ueno of visiting scholar and Dr. Hirotsugu Asano of lecturer in Professor Seo’s laboratory for kindly teaching me about animal experiments and DNA experiments and giving advice.

Finally, I thank each and every one of the members of Professor Seo’s laboratory.

References

1. Ferrara, N. Vascular endothelial growth factor. *Arterioscler Thromb Vasc Biol* **29**, 789-791 (2009).
2. Ferrara, N. & Davis-Smyth, T. The biology of vascular endothelial growth factor. *Endocr Rev* **18**, 4-25 (1997).
3. Potente, M., Gerhardt, H. & Carmeliet, P. Basic and therapeutic aspects of angiogenesis. *Cell* **146**, 873-887 (2011).
4. Hein, M. & Graver, S. Tumor cell response to bevacizumab single agent therapy in vitro. *Cancer Cell Int* **13**, 94 (2013).
5. Soker, S., Takashima, S., Miao, H.Q., Neufeld, G. & Klagsbrun, M. Neuropilin-1 is expressed by endothelial and tumor cells as an isoform-specific receptor for vascular endothelial growth factor. *Cell* **92**, 735-745 (1998).
6. Geretti, E., Shimizu, A. & Klagsbrun, M. Neuropilin structure governs VEGF and semaphorin binding and regulates angiogenesis. *Angiogenesis* **11**, 31-39 (2008).
7. Kawasaki, T*., et al.* A requirement for neuropilin-1 in embryonic vessel formation. *Development* **126**, 4895-4902 (1999).
8. Miao, H.Q., Lee, P., Lin, H., Soker, S. & Klagsbrun, M. Neuropilin-1 expression by tumor cells promotes tumor angiogenesis and progression. *FASEB J* **14**, 2532-2539 (2000).
9. Cao, Y*., et al.* VEGF exerts an angiogenesis-independent function in cancer cells to promote their malignant progression. *Cancer Res* **72**, 3912-3918 (2012).
10. Pellet-Many, C*., et al.* Neuropilin-1 mediates PDGF stimulation of vascular smooth muscle cell migration and signalling via p130Cas. *Biochem J* **435**, 609-618 (2011).
11. Snuderl, M*., et al.* Targeting placental growth factor/neuropilin 1 pathway inhibits growth and spread of medulloblastoma. *Cell* **152**, 1065-1076 (2013).
12. Van Cutsem, E*., et al.* Bevacizumab in Combination With Chemotherapy As First-Line Therapy in Advanced Gastric Cancer: A Biomarker Evaluation From the AVAGAST Randomized Phase III Trial. *J Clin Oncol* **30**, 2119-2127 (2012).
13. Beck, B*., et al.* A vascular niche and a VEGF-Nrp1 loop regulate the initiation and stemness of skin tumours. *Nature* **478**, 399-403 (2011).
14. Mountzios, G., Pentheroudakis, G. & Carmeliet, P. Bevacizumab and

micrometastases: revisiting the preclinical and clinical rollercoaster. *Pharmacol Ther* **141**, 117-124 (2013).

15. Herbst, R.S. & Sandler, A. Bevacizumab and erlotinib: a promising new approach to the treatment of advanced NSCLC. *Oncologist* **13**, 1166-1176 (2008).
16. Kawamura, H.*, et al.* Neuropilin-1 in regulation of VEGF-induced activation of p38MAPK and endothelial cell organization. *Blood* **112**, 3638-3649 (2008).
17. Bachelder, R.E.*, et al.* Vascular endothelial growth factor is an autocrine survival factor for neuropilin-expressing breast carcinoma cells. *Cancer Res* **61**, 5736-5740 (2001).
18. Wang, L., Mukhopadhyay, D. & Xu, X. C terminus of RGS-GAIP-interacting protein conveys neuropilin-1-mediated signaling during angiogenesis. *FASEB J* **20**, 1513-1515 (2006).
19. Fantin, A.*, et al.* The cytoplasmic domain of neuropilin 1 is dispensable for angiogenesis, but promotes the spatial separation of retinal arteries and veins. *Development* **138**, 4185-4191 (2011).
20. Cai, H. & Reed, R.R. Cloning and characterization of neuropilin-1-interacting protein: a PSD-95/Dlg/ZO-1 domain-containing protein that interacts with the cytoplasmic domain of neuropilin-1. *J Neurosci* **19**, 6519-6527 (1999).
21. Wang, L.*, et al.* RGS-GAIP-interacting protein controls breast cancer progression. *Mol Cancer Res* **8**, 1591-1600 (2010).
22. De Vries, L., Lou, X., Zhao, G., Zheng, B. & Farquhar, M.G. GIPC, a PDZ domain containing protein, interacts specifically with the C terminus of RGS-GAIP. *Proc Natl Acad Sci U S A* **95**, 12340-12345 (1998).
23. Ballmer-Hofer, K., Andersson, A.E., Ratcliffe, L.E. & Berger, P. Neuropilin-1 promotes VEGFR-2 trafficking through Rab11 vesicles thereby specifying signal output. *Blood* **118**, 816-826 (2011).
24. Muders, M.H.*, et al.* Targeting GIPC/synectin in pancreatic cancer inhibits tumor growth. *Clin Cancer Res* **15**, 4095-4103 (2009).
25. Chittenden, T.W.*, et al.* Therapeutic implications of GIPC1 silencing in cancer. *PLoS One* **5**, e15581 (2011).
26. Wu, D., Haruta, A. & Wei, Q. GIPC1 interacts with MyoGEF and promotes MDA-MB-231 breast cancer cell invasion. *J Biol Chem* **285**, 28643-28650 (2010).

27. Muders, M.H. Neuropilin and neuropilin associated molecules as new molecular targets in pancreatic adenocarcinoma. *Anticancer Agents Med Chem* **11**, 442-447 (2011).
28. Gao, Y., Li, M., Chen, W. & Simons, M. Synectin, syndecan-4 cytoplasmic domain binding PDZ protein, inhibits cell migration. *J Cell Physiol* **184**, 373-379 (2000).
29. Garnaas, M.K*., et al.* Syx, a RhoA guanine exchange factor, is essential for angiogenesis in Vivo. *Circ Res* **103**, 710-716 (2008).
30. Liu, M. & Horowitz, A. A PDZ-binding motif as a critical determinant of Rho guanine exchange factor function and cell phenotype. *Mol Biol Cell* **17**, 1880-1887 (2006).
31. De Toledo, M., Coulon, V., Schmidt, S., Fort, P. & Blangy, A. The gene for a new brain specific RhoA exchange factor maps to the highly unstable chromosomal region 1p36.2-1p36.3. *Oncogene* **20**, 7307-7317 (2001).
32. Nessling, M*., et al.* Candidate genes in breast cancer revealed by microarray-based comparative genomic hybridization of archived tissue. *Cancer Res* **65**, 439-447 (2005).
33. Croucher, D.R., Rickwood, D., Tactacan, C.M., Musgrove, E.A. & Daly, R.J. Cortactin modulates RhoA activation and expression of Cip/Kip cyclin-dependent kinase inhibitors to promote cell cycle progression in 11q13-amplified head and neck squamous cell carcinoma cells. *Mol Cell Biol* **30**, 5057-5070 (2010).
34. Vega, F.M. & Ridley, A.J. Rho GTPases in cancer cell biology. *FEBS Lett* **582**, 2093-2101 (2008).
35. Hu, W., Bellone, C.J. & Baldassare, J.J. RhoA stimulates p27(Kip) degradation through its regulation of cyclin E/CDK2 activity. *J Biol Chem* **274**, 3396-3401 (1999).
36. Mammoto, A., Huang, S., Moore, K., Oh, P. & Ingber, D.E. Role of RhoA, mDia, and ROCK in cell shape-dependent control of the Skp2-p27kip1 pathway and the G1/S transition. *J Biol Chem* **279**, 26323-26330 (2004).
37. Katayama, Y., Yamane, Y., Kitajima, Y., Yaoita, H., Touzyou, Y., Sakai, S. Malignant trichilemmal cyst secreting a cell adhesion factor. A case report for lymphatic metastases. *Hihuka-no Rinsho* **31**, 1721-1724 (1989).

38. Shimizu, A.*, et al.* ABL2/ARG tyrosine kinase mediates SEMA3F-induced RhoA inactivation and cytoskeleton collapse in human glioma cells. *J Biol Chem* **283**, 27230-27238 (2008).
39. Kizaka-Kondoh, S.*, et al.* Selective killing of hypoxia-inducible factor-1-active cells improves survival in a mouse model of invasive and metastatic pancreatic cancer. *Clin Cancer Res* **15**, 3433-3441 (2009).
40. Fukazawa, H., Mizuno, S. & Uehara, Y. A microplate assay for quantitation of anchorage-independent growth of transformed cells. *Anal Biochem* **228**, 83-90 (1995).
41. Parker, M.W., Xu, P., Li, X. & Vander Kooi, C.W. Structural basis for the selective vascular endothelial growth factor-A (VEGF-A) binding to neuropilin-1. *J Biol Chem* (2012).
42. Soker, S., Fidder, H., Neufeld, G. & Klagsbrun, M. Characterization of novel vascular endothelial growth factor (VEGF) receptors on tumor cells that bind VEGF165 via its exon 7-encoded domain. *J Biol Chem* **271**, 5761-5767 (1996).
43. Mamluk, R.*, et al.* Neuropilin-1 binds vascular endothelial growth factor 165, placenta growth factor-2, and heparin via its b1b2 domain. *J Biol Chem* **277**, 24818-24825 (2002).
44. Santarpia, L., Lippman, S.M. & El-Naggar, A.K. Targeting the MAPK-RAS-RAF signaling pathway in cancer therapy. *Expert Opin Ther Targets* **16**, 103-119 (2012).
45. Owonikoko, T.K. & Khuri, F.R. Targeting the PI3K/AKT/mTOR pathway: biomarkers of success and tribulation. *Am Soc Clin Oncol Educ Book* (2013).
46. Marx, R., Henderson, J., Wang, J. & Baraban, J.M. Tech: a RhoA GEF selectively expressed in hippocampal and cortical neurons. *J Neurochem* **92**, 850-858 (2005).
47. Mori, S.*, et al.* Anchorage-independent cell growth signature identifies tumors with metastatic potential. *Oncogene* **28**, 2796-2805 (2009).
48. Dallas, N.A.*, et al.* Neuropilin-2-mediated tumor growth and angiogenesis in pancreatic adenocarcinoma. *Clin Cancer Res* **14**, 8052-8060 (2008).
49. Goel, H.L. & Mercurio, A.M. VEGF targets the tumour cell. *Nat Rev Cancer* **13**, 871-882 (2013).
50. Seerapu, H.R.*, et al.* The cytoplasmic domain of neuropilin-1 regulates focal

adhesion turnover. *FEBS Lett* **587**, 3392-3399 (2013).

51. Fukasawa, M., Matsushita, A. & Korc, M. Neuropilin-1 interacts with integrin beta1 and modulates pancreatic cancer cell growth, survival and invasion. *Cancer Biol Ther* **6**, 1173-1180 (2007).
52. Soker, S., Miao, H.Q., Nomi, M., Takashima, S. & Klagsbrun, M. VEGF165 mediates formation of complexes containing VEGFR-2 and neuropilin-1 that enhance VEGF165-receptor binding. *J Cell Biochem* **85**, 357-368 (2002).
53. Pan, Q.*, et al.* Blocking neuropilin-1 function has an additive effect with anti-VEGF to inhibit tumor growth. *Cancer Cell* **11**, 53-67 (2007).
54. Rushing, E.C.*, et al.* Neuropilin-2: a novel biomarker for malignant melanoma? *Hum Pathol* (2011).
55. Dachsel, J.C.*, et al.* The Rho guanine nucleotide exchange factor Syx regulates the balance of dia and ROCK activities to promote polarized-cancer-cell migration. *Mol Cell Biol* **33**, 4909-4918 (2013).
56. Yoshida, A.*, et al.* VEGF-A/NRP1 stimulates GIPC1 and Syx complex formation to promote RhoA activation and proliferation in skin cancer cells. *Biol Open* (2015).
57. Kamai, T.*, et al.* Significant association of Rho/ROCK pathway with invasion and metastasis of bladder cancer. *Clin Cancer Res* **9**, 2632-2641 (2003).
58. Faried, A., Faried, L.S., Usman, N., Kato, H. & Kuwano, H. Clinical and prognostic significance of RhoA and RhoC gene expression in esophageal squamous cell carcinoma. *Ann Surg Oncol* **14**, 3593-3601 (2007).
59. Pan, Y.*, et al.* Expression of seven main Rho family members in gastric carcinoma. *Biochem Biophys Res Commun* **315**, 686-691 (2004).
60. Fritz, G., Just, I. & Kaina, B. Rho GTPases are over-expressed in human tumors. *Int J Cancer* **81**, 682-687 (1999).
61. Horiuchi, A.*, et al.* Up-regulation of small GTPases, RhoA and RhoC, is associated with tumor progression in ovarian carcinoma. *Lab Invest* **83**, 861-870 (2003).
62. Terada, M., Ohnishi, C., Ueno, N., Shimizu, A., Kanai, M., Seo-Kurokawa, M. Enhanced Expression of Fibriblast Growth Factor Receptor 3 in Human Skin Cancer Cells. *The Open Circulation and Vascular Journal* **2**, 30-36 (2009).
63. Berdeaux, R.L., Diaz, B., Kim, L. & Martin, G.S. Active Rho is localized to

podosomes induced by oncogenic Src and is required for their assembly and function. *J Cell Biol* **166**, 317-323 (2004).

64. Struckhoff, A.P., Rana, M.K. & Worthylake, R.A. RhoA can lead the way in tumor cell invasion and metastasis. *Front Biosci (Landmark Ed)* **16**, 1915-1926 (2011).
65. Katoh, M. Functional proteomics, human genetics and cancer biology of GIPC family members. *Exp Mol Med* **45**, e26 (2013).
66. Alattar, M., Omo, A., Elsharawy, M. & Li, J. Neuropilin-1 expression in squamous cell carcinoma of the oesophagus. *Eur J Cardiothorac Surg* **45**, 514-520 (2014).
67. Ruffini, F., D'Atri, S. & Lacal, P.M. Neuropilin-1 expression promotes invasiveness of melanoma cells through vascular endothelial growth factor receptor-2-dependent and -independent mechanisms. *Int J Oncol* **43**, 297-306 (2013).
68. Chen, L.*, et al.* The expression and significance of neuropilin-1 (NRP-1) on glioma cell lines and glioma tissues. *J Biomed Nanotechnol* **9**, 559-563 (2013).
69. Hirata, D.*, et al.* Involvement of epithelial cell transforming sequence-2 oncoantigen in lung and esophageal cancer progression. *Clin Cancer Res* **15**, 256-266 (2009).
70. Iyoda, M.*, et al.* Epithelial cell transforming sequence 2 in human oral cancer. *PLoS One* **5**, e14082 (2010).
71. Bennett, G., Sadlier, D., Doran, P.P., Macmathuna, P. & Murray, D.W. A functional and transcriptomic analysis of NET1 bioactivity in gastric cancer. *BMC Cancer* **11**, 50 (2011).
72. Hornstein, I.*, et al.* The haematopoietic specific signal transducer Vav1 is expressed in a subset of human neuroblastomas. *J Pathol* **199**, 526-533 (2003).
73. Lessey, E.C., Guilluy, C. & Burridge, K. From mechanical force to RhoA activation. *Biochemistry* **51**, 7420-7432 (2012).
74. Paez-Ribes, M.*, et al.* Antiangiogenic therapy elicits malignant progression of tumors to increased local invasion and distant metastasis. *Cancer Cell* **15**, 220-231 (2009).
75. Loges, S.*, et al.* Malignant cells fuel tumor growth by educating infiltrating leukocytes to produce the mitogen Gas6. *Blood* **115**, 2264-2273 (2009).
76. Geretti, E.*, et al.* A mutated soluble neuropilin-2 B domain antagonizes vascular

endothelial growth factor bioactivity and inhibits tumor progression. *Mol Cancer Res* **8**, 1063-1073 (2010).

77. Munaut, C.*, et al.* Vascular endothelial growth factor expression correlates with matrix metalloproteinases MT1-MMP, MMP-2 and MMP-9 in human glioblastomas. *Int J Cancer* **106**, 848-855 (2003).
78. Yan, G.*, et al.* Silencing RhoA inhibits migration and invasion through Wnt/beta-catenin pathway and growth through cell cycle regulation in human tongue cancer. *Acta Biochim Biophys Sin (Shanghai)* **46**, 682-690 (2014).
79. Hong, T.M.*, et al.* Targeting neuropilin 1 as an antitumor strategy in lung cancer. *Clin Cancer Res* **13**, 4759-4768 (2007).
80. Baba, T.*, et al.* Neuropilin-1 promotes unlimited growth of ovarian cancer by evading contact inhibition. *Gynecol Oncol* **105**, 703-711 (2007).
81. Hamerlik, P.*, et al.* Autocrine VEGF-VEGFR2-Neuropilin-1 signaling promotes glioma stem-like cell viability and tumor growth. *J Exp Med* **209**, 507-520 (2012).
82. Hu, B.*, et al.* Neuropilin-1 promotes human glioma progression through potentiating the activity of the HGF/SF autocrine pathway. *Oncogene* **26**, 5577-5586 (2007).
83. Osada, H.*, et al.* Overexpression of the neuropilin 1 (NRP1) gene correlated with poor prognosis in human glioma. *Anticancer Res* **24**, 547-552 (2004).
84. Gray, M.J.*, et al.* Therapeutic targeting of neuropilin-2 on colorectal carcinoma cells implanted in the murine liver. *J Natl Cancer Inst* **100**, 109-120 (2008).
85. Yasuoka, H.*, et al.* Neuropilin-2 expression in breast cancer: correlation with lymph node metastasis, poor prognosis, and regulation of CXCR4 expression. *BMC Cancer* **9**, 220 (2009).
86. Goel, H.L.*, et al.* VEGF/neuropilin-2 regulation of Bmi-1 and consequent repression of IGF-IR define a novel mechanism of aggressive prostate cancer. *Cancer Discov* **2**, 906-921 (2012).
87. Goel, H.L.*, et al.* GLI1 regulates a novel neuropilin-2/alpha6beta1 integrin based autocrine pathway that contributes to breast cancer initiation. *EMBO Mol Med* **5**, 488-508 (2013).
88. Kawakami, T.*, et al.* Neuropilin 1 and neuropilin 2 co-expression is significantly correlated with increased vascularity and poor prognosis in nonsmall cell lung

carcinoma. *Cancer* **95**, 2196-2201 (2002).

89. Lantuejoul, S*., et al.* Expression of VEGF, semaphorin SEMA3F, and their common receptors neuropilins NP1 and NP2 in preinvasive bronchial lesions, lung tumours, and cell lines. *J Pathol* **200**, 336-347 (2003).
90. Prahst, C*., et al.* Neuropilin-1-VEGFR-2 complexing requires the PDZ-binding domain of neuropilin-1. *J Biol Chem* **283**, 25110-25114 (2008).
91. Wey, J.S*., et al.* Overexpression of neuropilin-1 promotes constitutive MAPK signalling and chemoresistance in pancreatic cancer cells. *Br J Cancer* **93**, 233-241 (2005).
92. Hansel, D.E*., et al.* Expression of neuropilin-1 in high-grade dysplasia, invasive cancer, and metastases of the human gastrointestinal tract. *Am J Surg Pathol* **28**, 347-356 (2004).
93. Ochiumi, T*., et al.* Neuropilin-1 is involved in regulation of apoptosis and migration of human colon cancer. *Int J Oncol* **29**, 105-116 (2006).
94. Latil, A*., et al.* VEGF overexpression in clinically localized prostate tumors and neuropilin-1 overexpression in metastatic forms. *Int J Cancer* **89**, 167-171 (2000).
95. Yacoub, M*., et al.* Differential expression of the semaphorin 3A pathway in prostatic cancer. *Histopathology* **55**, 392-398 (2009).
96. Ghosh, S*., et al.* High levels of vascular endothelial growth factor and its receptors (VEGFR-1, VEGFR-2, neuropilin-1) are associated with worse outcome in breast cancer. *Hum Pathol* **39**, 1835-1843 (2008).
97. Staton, C.A*., et al.* Expression of class 3 semaphorins and their receptors in human breast neoplasia. *Histopathology* **59**, 274-282 (2011).
98. Matsushita, A., Gotze, T. & Korc, M. Hepatocyte growth factor-mediated cell invasion in pancreatic cancer cells is dependent on neuropilin-1. *Cancer Res* **67**, 10309-10316 (2007).
99. Muller, M.W*., et al.* Association of axon guidance factor semaphorin 3A with poor outcome in pancreatic cancer. *Int J Cancer* **121**, 2421-2433 (2007).
100. Weekes, C.D., Hegde, P., Xin, Y., Yu, R., Xiang, H., Beeram, M., Gore, L., Brachmann, R.K., Patnaik, A. A first-in-human phase I study to evaluate the fully human monoclonal antibody MNRP1685A (anti-NRP1) administered intravenously every three weeks in patients with advanced solid tumors. in

2010 American Society of Clinical Oncology Annual Meeting (Chicago, Illinois, 2010).

101. Xin, Y.*, et al.* Pharmacokinetic and pharmacodynamic analysis of circulating biomarkers of anti-NRP1, a novel antiangiogenesis agent, in two phase I trials in patients with advanced solid tumors. *Clin Cancer Res* **18**, 6040-6048 (2012).
102. Jia, H.*, et al.* Characterization of a bicyclic peptide neuropilin-1 (NP-1) antagonist (EG3287) reveals importance of vascular endothelial growth factor exon 8 for NP-1 binding and role of NP-1 in KDR signaling. *J Biol Chem* **281**, 13493-13502 (2006).
103. von Wronski, M.A.*, et al.* Tuftsin binds neuropilin-1 through a sequence similar to that encoded by exon 8 of vascular endothelial growth factor. *J Biol Chem* **281**, 5702-5710 (2006).
104. Starzec, A.*, et al.* Antiangiogenic and antitumor activities of peptide inhibiting the vascular endothelial growth factor binding to neuropilin-1. *Life Sci* **79**, 2370-2381 (2006).
105. Patra, C.R.*, et al.* Chemically Modified Peptides Targeting the PDZ Domain of GIPC as a Therapeutic Approach for Cancer. *ACS Chem Biol* (2012).